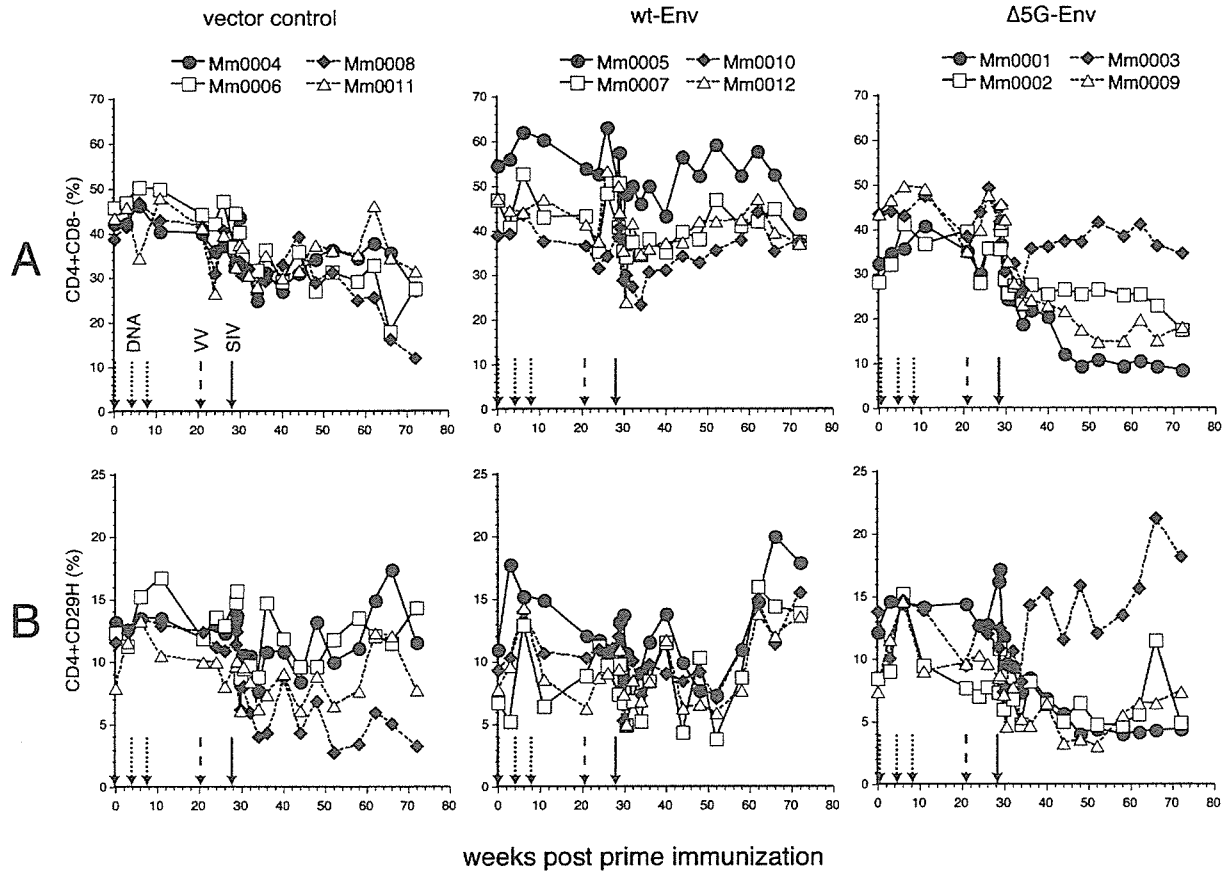

FIG. 6. $CD4^+$ T cells in PBMCs from rhesus macaques during immunization and after the challenge infection. A: Percentage of $CD4^+$ T cells in PBMCs; B: percentage of $CD4^+$ CD29high T cells in PBMCs.

were induced, with statistical significance ($P < 0.05$), in the control animals.

DISCUSSION

The heavily glycosylated structure of Env has been considered a main cause of chronically persistent viral replication and the pathogenicity of HIV/SIV, primarily because it potentially interferes with the development of the host immune response associated with protective immune functions, such as NAb and CTL (10, 36, 44). This characteristic constitutes the primary reason for the difficulty of developing effective vaccines. We therefore examined the efficacy of a deglycosylated-Env vaccine and compared it with the wt-Env vaccine. This study showed that quintuple deglycosylation neither improved the immunogenicity of the wt-Env vaccine nor elicited NAb against SIVmac239. This was in contrast to what occurred with Δ5G infection in rhesus macaques, because the host response elicited by Δ5G infection not only contained Δ5G infection but also protected the animals from SIVmac239 challenge infection (36). This study therefore suggested that an almost sterilizing immunity against SIVmac239 induced in Δ5G-infected animals could not be explained by the immunogenicity of Δ5G Env; instead, it is likely associated with the property of Δ5G as an attenuated virus. In fact, Δ5G was more neutralization-sensitive than SIVmac239 (36). Alternatively, the immunogenic property of Env in Δ5G could not successfully be duplicated by immunization with a Δ5G Env DNA prime-vaccinia virus boost regimen. Therefore, another immunization regimen might be able to elicit the protective immune response induced by Δ5G infection.

The Env vaccine is superior to other vaccines containing other viral proteins with respect to the induction of NAb; however, both the Δ5G Env vaccine and the wt-Env vaccine could not induce detectable NAb against either SIVmac239 or Δ5G. Instead, the wt-Env vaccine induced higher NAb against macrophage-tropic SIV than the Δ5G Env vaccine. Notably, this parameter most significantly correlated with the efficacies of the two Env vaccines. As Ab neutralized the macrophage-tropic variant 239/envMERT, which has only four separate amino acid substitutions distributed in *env* of SVmac239 (34), it might recognize unknown epitopes conserved between SIVmac239 and 239/envMERT. On the other hand, Δ5G Env may not sufficiently present this epitope due to mutations. Regarding the role of nonneutralizing Ab for the control of SIVmac239 infection, it is assumed that, as the neutralization assay did not necessarily reflect in vivo conditions, such nonneutralizing Ab with potential virus-binding ability may interfere with SIVmac239 infection in animals. Alternatively, Ab

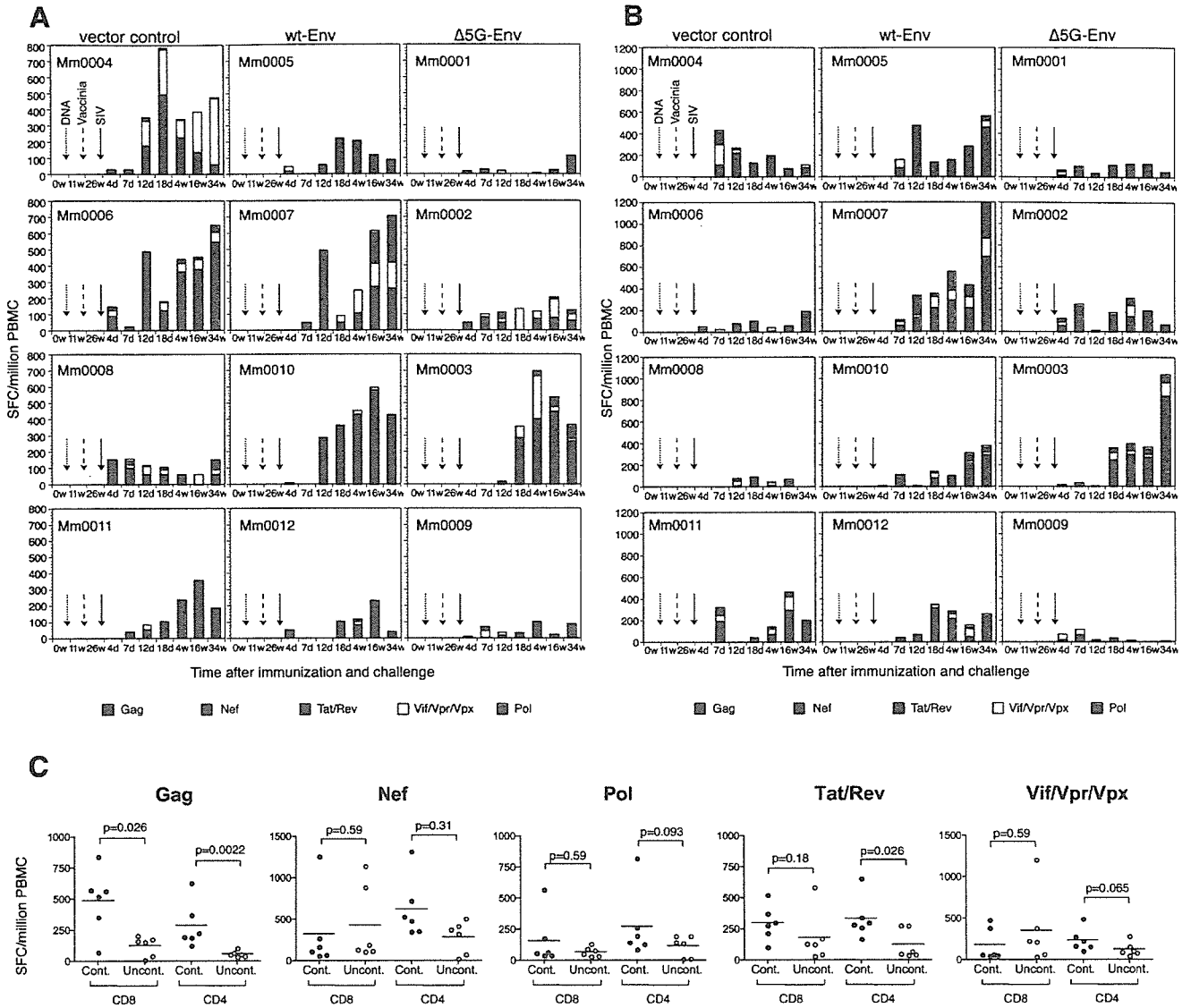

FIG. 7. SIV-specific $CD8^+$ T-cell and $CD4^+$ T-cell responses in 12 animals. A: SIV viral-protein-specific $CD8^+$ T cells in PBMCs were measured by ELISPOT assay for IFN-γ in three groups: vector controls, wt-Env vaccine group, and Δ5G Env vaccines. B: SIV viral-protein-specific $CD4^+$ T cells in PBMCs were measured by ELISPOT assay for IFN-γ in three groups. ELISPOT results of individual SIV proteins are colored as follows: Gag (red), Nef (green), Tat/Rev (blue), Vif/Vpr/Vpx (yellow), and Pol (pink). C: Comparison of cumulated $CD8^+$ T cells or $CD4^+$ T cells specific to the viral proteins Gag, Pol, Nef, Tat/Rev, and Vif/Vpr/VpX between SIV infection-controlled and uncontrolled animals. w, weeks; d, days.

might play a role in other effector functions, such as antibody-dependent cell-mediated cytotoxicity to eliminate the infected cells. The antibody-mediated enhancement of viral antigen processing and cross presentation is also a mechanism potentially related to the control of SIV infection in vivo (49).

Reduced immunogenicity in the Δ5G Env vaccine was also noted in cellular immunity. The levels of stimulation of antigen-specific $CD8^+$ T cells and $CD4^+$ T cells are MHC I and MHC II dependent, respectively. As the macaques in this study have different MHC haplotypes (data not shown), the magnitude and breadth of SIV-specific T cells should vary among the animals. Nevertheless, the magnitude of SU-specific $CD8^+$ T cells and $CD4^+$ T cells in PBMCs was greater in the wt-Env vaccine group than in the Δ5G Env vaccine group. Although the expression of SU by expressing plasmids and that of Env by the vaccinia virus vector elicited by either the wt-Env vaccine or Δ5G Env vaccine were indistinguishable in cultured cells (Fig. 2), wt-Env might persist longer than Δ5G Env in vaccinated animals. T-cell epitopes in the wt-Env vaccine might therefore be more efficiently presented on MHC molecules in antigen-presenting cells than in the Δ5G Env vaccine. Differences in glycosylation levels might also affect some processes in antigen-presenting cells associated with the presentation of T-cell epitopes in Env.

Taking all results together, Env glycosylation might affect the presentation of B-cell epitopes and T-cell epitopes required for Ab-mediated and T-cell-mediated immunities related to the control of SIV infection.

As seen in viral loads and SU-specific T cell levels after challenge infection (Fig. 3 and 5), the effect of vaccination was limited. That seemed related to the development of escape mutants. Therefore, distinctive cellular immune responses after the challenge infection were also implicated in the control of SIVmac239 replication. The magnitude of virus-specific $CD8^+$ T cells did not always correlate with the suppression of viral replication as reported previously (1, 6), particularly in vector controls (Fig. 5 and 7A); however, selected epitope-specific CTL responses might be associated with infection control. Gag-specific CTLs are such candidates, because a high magnitude of Gag-specific $CD8^+$ T cells was significantly elicited in five control animals (Fig. 7C). The magnitude of Gag- or Tat/Rev-specific $CD4^+$ T cells was statistically correlated with infection control (Fig. 7C). This may simply indicate a lower depletion of virus-specific $CD4^+$ T cells in animals with lower viral loads as reported previously (11). Alternatively, these virus-specific $CD4^+$ T cells may play an important role in protective immunity (39). Taken together, these results implicated the dominant role of selected epitope-specific $CD4^+$ T cells and $CD8^+$ T cells for the control of SIVmac239 infection.

The challenge virus that should be used has been an important issue in AIDS vaccine studies (8, 10, 12). Many studies have reported impressive efficacy in a pathogenic-SHIV macaque model (3, 4, 45, 46); however, pathogenic SHIVs use CXCR4 as a coreceptor, whereas the majority of clinical isolates of HIV-1 use CCR5 (13, 27). Therefore, the challenge virus for an AIDS vaccine study should be an R5 virus, such as SIV (10). Consistent with this concern, a DNA prime–modified-vaccinia virus Ankara boost regimen, inducing broad SIV-specific T-cell responses, reduced the initial viral replication but did not prevent disease progression against SIVmac239 challenge (18). Thus, vaccine studies using pathogenic SHIV should be reevaluated by using an R5 virus (10).

Matano et al. reported that a DNA prime-Sendai virus boost regimen induced the CTL-based control of SIVmac239 in rhesus macaques (27). This study demonstrated that a DNA prime-vaccinia virus WR boost regimen expressing only Env controlled the chronic infection of SIVmac239 in rhesus macaques. The relatively lower viral loads in macaques from Myanmar or Laos than in those of Indian origin might contribute to the control of SIVmac239 infection. Nevertheless, it is important that these two studies demonstrated the efficacies of the two vaccine regimens against highly pathogenic SIVmac239. In earlier studies, other R5 SIVs were used as a challenge virus for an efficacy study of vaccine candidates. An Env-based vaccine in vaccinia virus vector priming and subunit protein boosting protected cynomologous macaques against homologous SIVmne clone E11S (42). In recombinant modified vaccinia virus, Ankara viruses expressing Gag-Pol and/or Env exhibited vaccine efficacy because of reduced viremia and the increased survival of rhesus macaques infected with uncloned SIVsmE660 (41). Accordingly, the efficacy of vaccine candidates might be influenced by the experimental conditions. Thus, well-defined animal models with detailed virological, immunological, and genetic information and suitable challenge viruses are required for the evaluation of vaccine candidates and the development of an AIDS vaccine.

This study demonstrated the importance of Env as a component of the AIDS vaccine, and Env-specific $CD8^+$ and $CD4^+$ T cells and nonneutralizing Env-specific Ab were suggested as protective immunity components. Quintuple deglycosylation in Env reduced vaccine efficacy and Env-specific immune responses. Env may therefore be comprised of appropriate antigenic properties to elicit humoral and cellular immune responses required for protective immunity against homologous or allele-specific target SIV/HIV. These properties could be modified by the alteration of glycosylation.

In conclusion, although Env is an important immunogen for the AIDS vaccine, Env properties, including glycosylation, should be carefully considered to design vaccines specific to the targeted viruses.

ACKNOWLEDGMENTS

We thank Kayoko Ueda for excellent technical assistance.

This work was supported by AIDS research grants from the Health Sciences Research Grants, from the Ministry of Health, Labor, and Welfare in Japan, and from the Ministry of Education, Culture, Sports, Science and Technology in Japan.

REFERENCES

1. **Addo, M. M., X. G. Yu, A. Rathod, D. Cohen, R. L. Eldridge, D. Strick, M. N. Johnston, C. Corcoran, A. G. Wurcel, C. A. Fitzpatrick, M. E. Feeney, W. R. Rodriguez, N. Basgoz, R. Draenert, D. R. Stone, C. Brander, P. J. Goulder, E. S. Rosenberg, M. Altfeld, and B. D. Walker.** 2003. Comprehensive epitope analysis of human immunodeficiency virus type 1 (HIV-1)-specific T-cell responses directed against the entire expressed HIV-1 genome demonstrate broadly directed responses, but no correlation to viral load. J. Virol. **77**:2081–2092.
2. **Allen, T. M., and D. I. Watkins.** 2001. New insights into evaluating effective T-cell responses to HIV. AIDS **15**(Suppl. 5):S117–S126.
3. **Amara, R. R., F. Villinger, J. D. Altman, S. L. Lydy, S. P. O'Neil, S. I. Staprans, D. C. Montefiori, Y. Xu, J. G. Herndon, L. S. Wyatt, M. A. Candido, N. L. Kozyr, P. L. Earl, J. M. Smith, H. L. Ma, B. D. Grimm, M. L. Hulsey, J. Miller, H. M. McClure, J. M. McNicholl, B. Moss, and H. L. Robinson.** 2001. Control of a mucosal challenge and prevention of AIDS by a multiprotein DNA/MVA vaccine. Science **292**:69–74.
4. **Barouch, D. H., S. Santra, J. E. Schmitz, M. J. Kuroda, T. M. Fu, W. Wagner, M. Bilska, A. Craiu, X. X. Zheng, G. R. Krivulka, K. Beaudry, M. A. Lifton, C. E. Nickerson, W. L. Trigona, K. Punt, D. C. Freed, L. Guan, S. Dubey, D. Casimiro, A. Simon, M. E. Davies, M. Chastain, T. B. Strom, R. S. Gelman, D. C. Montefiori, M. G. Lewis, E. A. Emini, J. W. Shiver, and N. L. Letvin.** 2000. Control of viremia and prevention of clinical AIDS in rhesus monkeys by cytokine-augmented DNA vaccination. Science **290**:486–492.
5. **Berger, E. A., P. M. Murphy, and J. M. Farber.** 1999. Chemokine receptors as HIV-1 coreceptors: roles in viral entry, tropism, and disease. Annu. Rev. Immunol. **17**:657–700.
6. **Betts, M. R., D. R. Ambrozak, D. C. Douek, S. Bonhoeffer, J. M. Brenchley, J. P. Casazza, R. A. Koup, and L. J. Picker.** 2001. Analysis of total human immunodeficiency virus (HIV)-specific CD4(+) and CD8(+) T-cell responses: relationship to viral load in untreated HIV infection. J. Virol. **75**:11983–11991.
7. **Burton, D. R.** 2002. Antibodies, viruses and vaccines. Nat. Rev. Immunol. **2**:706–713.
8. **Burton, D. R., R. C. Desrosiers, R. W. Doms, W. C. Koff, P. D. Kwong, J. P. Moore, G. J. Nabel, J. Sodroski, I. A. Wilson, and R. T. Wyatt.** 2004. HIV vaccine design and the neutralizing antibody problem. Nat. Immunol. **5**:233–236.
9. **Chapman, B. S., R. M. Thayer, K. A. Vincent, and N. L. Haigwood.** 1991. Effect of intron A from human cytomegalovirus (Towne) immediate-early gene on heterologous expression in mammalian cells. Nucleic Acids Res. **19**:3979–3986.
10. **Desrosiers, R. C.** 2004. Prospects for an AIDS vaccine. Nat. Med. **10**:221–223.
11. **Douek, D. C., J. M. Brenchley, M. R. Betts, D. R. Ambrozak, B. J. Hill, Y. Okamoto, J. P. Casazza, J. Kuruppu, K. Kunstman, S. Wolinsky, Z. Grossman, M. Dybul, A. Oxenius, D. A. Price, M. Connors, and R. A. Koup.** 2002. HIV preferentially infects HIV-specific CD4+ T cells. Nature **417**:95–98.
12. **Emini, E. A., and W. C. Koff.** 2004. AIDS/HIV. Developing an AIDS vaccine: need, uncertainty, hope. Science **304**:1913–1914.
13. **Feinberg, M. B., and J. P. Moore.** 2002. AIDS vaccine models: challenging challenge viruses. Nat Med. **8**:207–210.
14. **Gardner, M. B.** 2003. Simian AIDS: an historical perspective. J. Med. Primatol. **32**:180–186.
15. **Gotoh, H., T. Shioda, Y. Sakai, K. Mizumoto, and H. Shibuta.** 1989. Rescue

of Sendai virus from viral ribonucleoprotein-transfected cells by infection with recombinant vaccinia viruses carrying Sendai virus L and P/C genes. Virology **171**:434–443.
16. **Haigwood, N. L., and L. Stamatatos.** 2003. Role of neutralizing antibodies in HIV infection. AIDS **17**(Suppl. 4):S67–S71.
17. **Hirsch, V. M.** 2004. What can natural infection of African monkeys with simian immunodeficiency virus tell us about the pathogenesis of AIDS? AIDS Rev. **6**:40–53.
18. **Horton, H., T. U. Vogel, D. K. Carter, K. Vielhuber, D. H. Fuller, T. Shipley, J. T. Fuller, K. J. Kunstman, G. Sutter, D. C. Montefiori, V. Erfle, R. C. Desrosiers, N. Wilson, L. J. Picker, S. M. Wolinsky, C. Wang, D. B. Allison, and D. I. Watkins.** 2002. Immunization of rhesus macaques with a DNA prime/modified vaccinia virus Ankara boost regimen induces broad simian immunodeficiency virus (SIV)-specific T-cell responses and reduces initial viral replication but does not prevent disease progression following challenge with pathogenic SIVmac239. J. Virol. **76**:7187–7202.
19. **Johnson, R. P., R. L. Glickman, J. Q. Yang, A. Kaur, J. T. Dion, M. J. Mulligan, and R. C. Desrosiers.** 1997. Induction of vigorous cytotoxic T-lymphocyte responses by live attenuated simian immunodeficiency virus. J. Virol. **71**:7711–7718.
20. **Johnson, W. E., J. D. Lifson, S. M. Lang, R. P. Johnson, and R. C. Desrosiers.** 2003. Importance of B-cell responses for immunological control of variant strains of simian immunodeficiency virus. J. Virol. **77**:375–381.
21. **Johnson, W. E., H. Sanford, L. Schwall, D. R. Burton, P. W. Parren, J. E. Robinson, and R. C. Desrosiers.** 2003. Assorted mutations in the envelope gene of simian immunodeficiency virus lead to loss of neutralization resistance against antibodies representing a broad spectrum of specificities. J. Virol. **77**:9993–10003.
22. **Kano, M., T. Matano, A. Kato, H. Nakamura, A. Takeda, Y. Suzaki, Y. Ami, K. Terao, and Y. Nagai.** 2002. Primary replication of a recombinant Sendai virus vector in macaques. J. Gen. Virol. **83**:1377–1386.
23. **Kano, M., T. Matano, H. Nakamura, A. Takeda, A. Kato, K. Ariyoshi, K. Mori, T. Sata, and Y. Nagai.** 2000. Elicitation of protective immunity against simian immunodeficiency virus infection by a recombinant Sendai virus expressing the Gag protein. AIDS **14**:1281–1282.
24. **Letvin, N. L., J. E. Schmitz, H. L. Jordan, A. Seth, V. M. Hirsch, K. A. Reimann, and M. J. Kuroda.** 1999. Cytotoxic T lymphocytes specific for the simian immunodeficiency virus. Immunol. Rev. **170**:127–134.
25. **Lifson, J. D., M. A. Nowak, S. Goldstein, J. L. Rossio, A. Kinter, G. Vasquez, T. A. Wiltrout, C. Brown, D. Schneider, L. Wahl, A. L. Lloyd, J. Williams, W. R. Elkins, A. S. Fauci, and V. M. Hirsch.** 1997. The extent of early viral replication is a critical determinant of the natural history of simian immunodeficiency virus infection. J. Virol. **71**:9508–9514.
26. **Matano, T., M. Kano, T. Odawara, H. Nakamura, A. Takeda, K. Mori, T. Sato, and Y. Nagai.** 2000. Induction of protective immunity against pathogenic simian immunodeficiency virus by a foreign receptor-dependent replication of an engineered avirulent virus. Vaccine **18**:3310–3318.
27. **Matano, T., M. Kobayashi, H. Igarashi, A. Takeda, H. Nakamura, M. Kano, C. Sugimoto, K. Mori, A. Iida, T. Hirata, M. Hasegawa, T. Yuasa, M. Miyazawa, Y. Takahashi, M. Yasunami, A. Kimura, D. H. O'Connor, D. I. Watkins, and Y. Nagai.** 2004. Cytotoxic T lymphocyte-based control of simian immunodeficiency virus replication in a preclinical AIDS vaccine trial. J Exp. Med. **199**:1709–1718.
28. **McMichael, A. J., and S. L. Rowland-Jones.** 2001. Cellular immune responses to HIV. Nature **410**:980–987.
29. **Means, R. E., T. Greenough, and R. C. Desrosiers.** 1997. Neutralization sensitivity of cell culture-passaged simian immunodeficiency virus. J. Virol. **71**:7895–7902.
30. **Means, R. E., T. Matthews, J. A. Hoxie, M. H. Malim, T. Kodama, and R. C. Desrosiers.** 2001. Ability of the V3 loop of simian immunodeficiency virus to serve as a target for antibody-mediated neutralization: correlation of neutralization sensitivity, growth in macrophages, and decreased dependence on CD4. J. Virol. **75**:3903–3915.
31. **Mellors, J. W., L. A. Kingsley, C. R. Rinaldo, Jr., J. A. Todd, B. S. Hoo, R. P. Kokka, and P. Gupta.** 1995. Quantitation of HIV-1 RNA in plasma predicts outcome after seroconversion. Ann. Intern. Med. **122**:573–579.
32. **Moore, J. P., S. G. Kitchen, P. Pugach, and J. A. Zack.** 2004. The CCR5 and CXCR4 coreceptors—central to understanding the transmission and pathogenesis of human immunodeficiency virus type 1 infection. AIDS Res. Hum. Retrovir. **20**:111–126.
33. **Mori, K., D. J. Ringler, and R. C. Desrosiers.** 1993. Restricted replication of simian immunodeficiency virus strain 239 in macrophages is determined by Env but is not due to restricted entry. J. Virol. **67**:2807–2814.
34. **Mori, K., D. J. Ringler, T. Kodama, and R. C. Desrosiers.** 1992. Complex determinants of macrophage tropism in Env of simian immunodeficiency virus. J. Virol. **66**:2067–2075.
35. **Mori, K., M. Rosenzweig, and R. C. Desrosiers.** 2000. Mechanisms for adaptation of simian immunodeficiency virus to replication in alveolar macrophages. J. Virol. **74**:10852–10859.
36. **Mori, K., Y. Yasutomi, S. Ohgimoto, T. Nakasone, S. Takamura, T. Shioda, and Y. Nagai.** 2001. Quintuple deglycosylation mutant of simian immunodeficiency virus SIVmac239 in rhesus macaques: robust primary replication, tightly contained chronic infection, and elicitation of potent immunity against the parental wild-type strain. J. Virol. **75**:4023–4028.
37. **Mori, K., Y. Yasutomi, S. Sawada, F. Villinger, K. Sugama, B. Rosenwith, J. L. Heeney, K. Uberla, S. Yamazaki, A. A. Ansari, and H. Rubsamen-Waigmann.** 2000. Suppression of acute viremia by short-term postexposure prophylaxis of simian/human immunodeficiency virus SHIV-RT-infected monkeys with a novel reverse transcriptase inhibitor (GW420867) allows for development of potent antiviral immune responses resulting in efficient containment of infection. J. Virol. **74**:5747–5753.
38. **Munch, J., N. Adam, N. Finze, N. Stolte, C. Stahl-Hennig, D. Fuchs, P. Ten Haaft, J. L. Heeney, and F. Kirchhoff.** 2001. Simian immunodeficiency virus in which *nef* and U3 sequences do not overlap replicates efficiently in vitro and in vivo in rhesus macaques. J. Virol. **75**:8137–8146.
39. **Norris, P. J., and E. S. Rosenberg.** 2001. Cellular immune response to human immunodeficiency virus. AIDS **15**(Suppl. 2):S16–S21.
40. **Ohgimoto, S., T. Shioda, K. Mori, E. E. Nakayama, H. Hu, and Y. Nagai.** 1998. Location-specific, unequal contribution of the N glycans in simian immunodeficiency virus gp120 to viral infectivity and removal of multiple glycans without disturbing infectivity. J. Virol. **72**:8365–8370.
41. **Ourmanov, I., C. R. Brown, B. Moss, M. Carroll, L. Wyatt, L. Pletneva, S. Goldstein, D. Venzon, and V. M. Hirsch.** 2000. Comparative efficacy of recombinant modified vaccinia virus Ankara expressing simian immunodeficiency virus (SIV) Gag-Pol and/or Env in macaques challenged with pathogenic SIV. J. Virol. **74**:2740–2751.
42. **Polacino, P., V. Stallard, J. E. Klaniecki, D. C. Montefiori, A. J. Langlois, B. A. Richardson, J. Overbaugh, W. R. Morton, R. E. Benveniste, and S. L. Hu.** 1999. Limited breadth of the protective immunity elicited by simian immunodeficiency virus SIVmne gp160 vaccines in a combination immunization regimen. J. Virol. **73**:618–630.
43. **Reeves, J. D., and R. W. Doms.** 2002. Human immunodeficiency virus type 2. J. Gen. Virol. **83**:1253–1265.
44. **Reitter, J. N., R. E. Means, and R. C. Desrosiers.** 1998. A role for carbohydrates in immune evasion in AIDS. Nat. Med. **4**:679–684.
45. **Robinson, H. L., D. C. Montefiori, R. P. Johnson, K. H. Manson, M. L. Kalish, J. D. Lifson, T. A. Rizvi, S. Lu, S. L. Hu, G. P. Mazzara, D. L. Panicali, J. G. Herndon, R. Glickman, M. A. Candido, S. L. Lydy, M. S. Wyand, and H. M. McClure.** 1999. Neutralizing antibody-independent containment of immunodeficiency virus challenges by DNA priming and recombinant pox virus booster immunizations. Nat. Med. **5**:526–534.
46. **Rose, N. F., P. A. Marx, A. Luckay, D. F. Nixon, W. J. Moretto, S. M. Donahoe, D. Montefiori, A. Roberts, L. Buonocore, and J. K. Rose.** 2001. An effective AIDS vaccine based on live attenuated vesicular stomatitis virus recombinants. Cell **106**:539–549.
47. **Stebbing, J., B. Gazzard, and D. C. Douek.** 2004. Where does HIV live? N. Engl. J. Med. **350**:1872–1880.
48. **Sugimoto, C., K. Tadakuma, I. Otani, T. Moritoyo, H. Akari, F. Ono, Y. Yoshikawa, T. Sata, S. Izumo, and K. Mori.** 2003. *nef* gene is required for robust productive infection by simian immunodeficiency virus of T-cell-rich paracortex in lymph nodes. J. Virol. **77**:4169–4180.
49. **Villinger, F., A. E. Mayne, P. Bostik, K. Mori, P. E. Jensen, R. Ahmed, and A. A. Ansari.** 2003. Evidence for antibody-mediated enhancement of simian immunodeficiency virus (SIV) Gag antigen processing and cross presentation in SIV-infected rhesus macaques. J. Virol. **77**:10–24.
50. **Watanabe, M. E.** 2003. Skeptical scientists skewer VaxGen statistics. Nat. Med. **9**:376.
51. **Wei, X., J. M. Decker, S. Wang, H. Hui, J. C. Kappes, X. Wu, J. F. Salazar-Gonzalez, M. G. Salazar, J. M. Kilby, M. S. Saag, N. L. Komarova, M. A. Nowak, B. H. Hahn, P. D. Kwong, and G. M. Shaw.** 2003. Antibody neutralization and escape by HIV-1. Nature **422**:307–312.
52. **Yu, D., T. Shioda, A. Kato, M. K. Hasan, Y. Sakai, and Y. Nagai.** 1997. Sendai virus-based expression of HIV-1 gp120: reinforcement by the V(−) version. Genes Cells **2**:457–466.

D. Shichi
E.F. Kikkawa
M. Ota
Y. Katsuyama
A. Kimura
A. Matsumori
J.K. Kulski
T.K. Naruse
H. Inoko

The haplotype block, *NFKBIL1-ATP6V1G2-BAT1-MICB-MICA*, within the class III – class I boundary region of the human major histocompatibility complex may control susceptibility to hepatitis C virus-associated dilated cardiomyopathy

Key words:
dilated cardiomyopathy (DCM); hepatitis C virus (HCV); human leukocyte antigen region; hypertrophic cardiomyopathy (HCM); microsatellite; single nucleotide polymorphism (SNP)

Acknowledgments
We are grateful to Drs A. Hasegawa, R. Nagai, T. Izumi, N. Aoyama, K. Yamauchi-Takihara, Y. Sato, Y. Takatsu, S. Maruyama, E. Matsuyama, K. Nakamura, T. Ohe, Y. Sakai, H. Kotoura, M. Matsuzaki, and T. Yamamura for their contributions in clinical evaluation and blood sampling from patients with HCV-DCM or HCV-HCM. This study was supported by grants as follows: Japanese Ministry of Health and Welfare, Mitsui Life Social Welfare Foundation, and Tokai University, School of Medicine Research Aid 2002.

Abstract: Cardiomyopathy is a heart muscle disease with impaired stretch response that can result in severe heart failure and sudden death. A small proportion of hepatitis C virus (HCV)-infected patients may be predisposed to develop dilated cardiomyopathy (DCM) and hypertrophic cardiomyopathy (HCM). The molecular mechanisms involved in the predisposition remain unknown due in part to the lack of information on their genetic background. Because the human leukocyte antigen (HLA) region has a pivotal role in controlling the susceptibility to HCV-induced liver disease, we hypothesized that particular *HLA* alleles and/or non-*HLA* gene alleles within the human major histocompatibility complex (MHC) genomic region might control the predisposition to HCV-associated DCM (HCV-DCM) and/or HCV-associated HCM (HCV-HCM). Here, we present mapping results of the MHC-related susceptibility gene locus for HCV-associated cardiomyopathy by analyzing microsatellite and single nucleotide polymorphism markers. To delineate the susceptibility locus, we genotyped 44 polymorphic markers scattered across the entire MHC region in a total of 59 patients (21 HCV-DCM and 38 HCV-HCM) and 120 controls. We mapped HCV-DCM susceptibility to a non-*HLA* gene locus spanning from *NFKBIL1* to *MICA* gene loci within the MHC class III – class I boundary region. Our results showed that HCV-DCM was more strongly associated with alleles of the non-*HLA* genes rather than the *HLA* genes themselves. In addition, no significant association was found between the MHC markers and HCV-HCM. This marked difference in the MHC-related disease susceptibility for HCV-associated cardiomyopathy strongly suggests that the development of HCV-DCM and HCV-HCM is under the control of different pathogenic mechanisms.

Hepatitis C virus (HCV) is a major pathogen of liver disease (1). It also infects various extrahepatic tissues (2) and causes clinical manifestations that do not originate from hepatopathy (3). The extrahepatic manifestation includes cardiomyopathy that is defined as a heart muscle disease with impaired stretch response that can result in heart failure and sudden death (4–7). Dilated cardiomyopathy (DCM) and hypertrophic cardiomyopathy (HCM) are two major clinical phenotypes of the HCV-associated cardiomyopathy. DCM is characterized by chamber dilation with contractile dysfunction. In contrast, HCM exhibits cardiac hypertrophy with diastolic ventricular failure. Not all of the patients infected with HCV develop cardiomyopathy, and there is a report showing DCM and HCM can be found in 5.7 and 6.6%, respectively, of random patients with positive HCV antibody (8).

Authors' affiliation:

D. Shichi[1,2],
E.F. Kikkawa[1],
M. Ota[3],
Y. Katsuyama[3],
A. Kimura[2,4],
A. Matsumori[5],
J.K. Kulski[1,6],
T.K. Naruse[1],
H. Inoko[1]

[1]Department of Basic Medical Science and Molecular Medicine, Tokai University School of Medicine, Isehara, Kanagawa, Japan

[2]Department of Molecular Pathogenesis, Medical Research Institute, Tokyo Medical and Dental University, Chiyoda-ku, Tokyo, Japan

[3]Department of Legal Medicine, Shinshu University School of Medicine, Matsumoto, Nagano, Japan

[4]Laboratory of Genome Diversity, School of Biomedical Science, Tokyo Medical and Dental University, Chiyoda-ku, Tokyo, Japan

[5]Department of Cardiovascular Medicine, Kyoto University Graduate School of Medicine, Sakyo-ku, Kyoto, Japan

[6]Center for Bioinformatics and Biological Computing, Murdoch University School of Information Technology, Murdoch, Western Australia, Australia

Correspondence to:
Hidetoshi Inoko, PhD, MD
Department of Basic Medical Science and Molecular Medicine
Tokai University School of Medicine
Bohseidai, Isehara
Kanagawa 259-1193
Japan
Tel.:
+81 463 93 1121x2312
Fax: +81 463 94 8884
e-mail: hinoko@is.icc.u-tokai.ac.jp

Received 3 March 2005, revised 24 May 2005, accepted for publication 30 May 2005

doi: 10.1111/j.1399-0039.2005.00457.x

Tissue Antigens 2005: **66:** 200–208
Printed in Singapore.

This epidemiological study suggests that there may be predisposing factors in the virus and/or infected host, which affect the clinical outcome of viral pathogenesis. To date, it is not clear whether or not there are cardiotropic HCV strains, and how they can escape cellular immune responses. It also remains unknown which genetic factors would predispose the infected patients to develop HCV-associated DCM (HCV-DCM) or HCV-associated HCM (HCV-HCM).

Human major histocompatibility complex (MHC), also called human leukocyte antigen (HLA) complex, on chromosome 6p21.3 plays a pivotal role in antiviral defense as a genetic factor controlling the immune response (9). The MHC genomic region consists of densely packed gene clusters including the *HLA* genes (10), the most polymorphic genes in the human genome (11–13). In addition to the classical and non-classical *HLA* class I and class II genes that regulate the cell-mediated immune response, there are at least 126 non-*HLA* coding genes within the MHC genomic region, which might affect acute and/or chronic viral infection and susceptibility to disease. Of particular interest are the 60 non-*HLA* coding genes within the MHC class III region, many of which have a role in regulating inflammation or have strong associations with susceptibility to diseases, such as rheumatoid arthritis (14), myocardial infarction (15), malaria (16), septic shock (17), and Ehlers – Danlos syndrome (18). The statistical analysis of extensive linkage disequilibrium (LD) across the entire 3.6-Mb MHC region has resulted in the detection and categorization of population-specific HLA haplotypes based on the allelic distribution and allelic combination of different MHC genes (19–21).

Although HCV appears to infect humans regardless of their *HLA* genotypes, the classical *HLA* alleles may determine the natural history of the viral infection in the post-infectious stage, such as viral resolution, the progression/suppression of persistent infection, and liver disease. For example, *HLA-B*44-DRB1*1302-DQB1*0604* haplotype carriers remain asymptomatic, whereas *B*54-DRB1*0405-DQB1*0401* carriers tend to develop chronic liver disease (22). Therefore, we hypothesized that either particular *HLA* or non-*HLA* gene alleles might regulate the development of DCM and/or HCM after HCV infection. In this study, we undertook genotyping to map the HLA-linked susceptibility loci for HCV-DCM and HCV-HCM in order to better understand the immuno-genetic factors controlling the clinical outcome of chronic HCV infection. This is the first genetic study to demonstrate that a non-*HLA* locus within the MHC class III – class I boundary region may confer the susceptibility to HCV-DCM in Japanese.

Materials and methods

Subjects

Diagnosis of DCM and HCM was based on the criteria of the Japan Research Committee on Idiopathic Cardiomyopathy developed with guidance from the report by the 1980 World Health Organization/International Society and Federation of Cardiology task force on the definition and classification of cardiomyopathies (23, 24). Among the Japanese patients who conformed with the diagnostic criteria, a total of 59 patients positive for the anti-HCV antibody (21 patients of HCV-DCM and 38 patients of HCV-HCM) were enrolled in this study along with 120 healthy controls after obtaining informed consent. All of them were genetically unrelated. Genomic DNAs were extracted by the guanidine hydrochloride method from each peripheral blood sample. The study protocol was approved by the Ethics Reviewing Committee of Tokai University School of Medicine.

Genotyping for microsatellite polymorphisms

Genotyping was performed with 19 microsatellite markers located within the MHC genomic region to identify the susceptibility locus for HCV-DCM and/or HCV-HCM. The marker order, genomic distances, and primer sequence were described previously (25, 26). Each forward primer was synthesized by labeling at the 5′ end with a fluorochrome 6-FAM, HEX, or TET (Applied Biosystems, Foster City, CA, USA). The fragment samples were mixed with formamide-containing stop buffer and GeneScan-500 ROX size standard (Applied Biosystems) and separated by GeneScan system on a 377 DNA sequencer (Applied Biosystems). Repeat fragment sizes were assigned by GENOTYPER software (Applied Biosystems).

Genotyping for two classical *HLA* genes, *HLA-B*, and *HLA-Cw*

The high resolution typing for *HLA-B* and *HLA-Cw* was performed by the sequence-based typing (SBT) method according to standard procedures (Forensic Analytical, Hayward, CA, USA). The MATCHMAKER allele Identification program (Applied Biosystems) was used to assign the *HLA* alleles.

Genotyping for five non-*HLA* genes, *TNF*, *LTA*, *NFKBIL1*, *ATP6V1G2*, and *BAT1*

A total of 23 single nucleotide polymorphisms (SNPs) as shown in Fig. 2 were examined in this study. The tumor necrosis factor (*TNF*), nuclear factor of kappa light polypeptide gene enhancer in B-cells inhibitor-like 1 also known as *IκBL* (*NFKBIL1*), and HLA-B associated transcript 1 (*BAT1*) genes were genotyped by the direct sequencing method using the primer sets as previously reported

Primers used for genotyping the candidate genes, *LTA* and *ATP6V1G2*

Gene	Target	Name	Primer sequence (5′–3′)	Length (mer)	Product (bp)	Annealing (°C)
LTA						
	+80C/A	LTA1F2	CTC CAC ACA GCA GGT GAG G	19	172	58
		LTA1R2	CCA AAA CCA AAC CCA CCA AG	20		
	+252A/G	LTA1F	GCT TCG TGC TTT GGA CTA CC	20	714	60
		LTA3R	GGG AGG TCA GGT GGA TGT TTA C	22		
ATP6V1G2 (ATP6G)						
	Exon1	ATPex1F	AGG AGG ACC AGT CAT CAA TAG GAG	24	306	66
		ATPex1R	CTA AGG GAG GAA AGA GGA GAC TCA	24		
	Exon2 and *+760A/T* (rs2523502)	ATPex2F	GGG ACT GAC TCC TGC TAT TAC ATT G	25	247	64
		ATPex2R	CAC CCT TAC ACA CCT CAC TAG ATG C	25		
	Exon3 and *+1222C/T* (rs2239705)	ATPex3F	CTT TCT TCT AGG CTT TGT TTC AGG A	25	527	62
		ATPex3R	CAA ATT TCA CAG AGG GTT TAG GTG A	25		

Table 1

(27–29). The *ATP6V1G2* gene was analyzed for all exons in addition to two intronic SNPs, *ATP6V1G2*+760* (dbSNP accession number rs2523502) and *ATP6V1G2*+1222* (rs2239705), through the direct sequencing method by primer sets as listed in Table 1. Cycle sequencing was performed using the Big-Dye Terminator system (Applied Biosystems). The sequencing analysis was conducted with an ABI Prism 377 DNA sequencer (Applied Biosystems). The genotypes were determined by manual comparison of patients' sequences with a public reference sequence (GeneBank accession number AB063177). In the *LTA* (lymphotoxin-alpha) gene, alleles carried at +80 and +252 (30) were screened by the PCR-single strand conformation polymorphism analysis and the PCR-restriction fragment length polymorphism method at the *Nco* I site, respectively.

Statistical analysis

The Hardy – Weinberg equilibrium distribution for the SNPs and their haplotypes was assessed by Fisher's exact test with Bonferroni's inequality method. The statistical significance was assigned at P and corrected P (Pc) values of less than 0.05. The strength of the association with HCV-DCM and/or HCV-HCM was evaluated by odds ratio (OR) with 95% confidence interval. The R package 'haplo.stats' (http://www.r-project.org/) was used to evaluate haplotype structure carrying the disease-associated markers around the candidate region. On the basis of the haplotype structure, the LD around the candidate region was measured in both patients and controls with two LD coefficients, Lewontin's D' and Hill's r^2, obtained from the R package 'genetics' (http://www.r-project.org/).

Results

Susceptibility gene mapping for HCV-associated cardiomyopathy with microsatellite markers encompassing the MHC genomic region

In an initial association analysis, we carried out a region-wide scan using 19 microsatellite markers dispersed throughout the MHC region. The multipoint analysis displayed different association profiles between HCV-DCM and HCV-HCM as illustrated in Fig. 1. In the analysis of HCV-DCM, significant associations were observed with two markers positioned around the boundary region between class III and class I: *STR-MICA*183* (OR = 4.59, $P = 0.005$, $Pc = 0.026$) and *C1-4-1*225* (OR = 3.57, $P = 0.006$, $Pc = 0.042$). Because LD of microsatellite markers usually extend some hundred kb, we considered a approximately 300-kb interval as a potential susceptibility locus for HCV-DCM, which contains 9 genes as follows; *TNF*, *LTA*, *NFKBIL1*, *ATP6V1G2* (vacuolar ATP synthase subunit G 2; also known as *ATP6G*), *BAT1*, *MICB* (MHC class I′ chain-related protein B), *MICA* (MHC class I chain-related gene A protein), *HLA-B*, and *HLA-Cw* (Fig. 2). In clear contrast, there were no significant associations between the HCV-HCM and the microsatellite markers in the MHC region.

Screening of SNP in association with the susceptibility to HCV-DCM in seven candidate genes

To identify the susceptibility gene, we examined SNPs in each of the candidate genes and compared their individual as well as their combined (haplotype) frequencies between the HCV-DCM patients and control individuals (Table 2). Of 16 *HLA-B* and 9 *HLA-Cw* alleles assigned by SBT method in HCV-DCM patients, *HLA-B*0702* (OR = 3.96, $P = 0.022$, $Pc = 0.356$) and *HLA-Cw*0702* (OR = 3.00, $P = 0.019$, $Pc = 0.192$) showed marginally significant associations with HCV-DCM. Additionally, of the seven non-*HLA* genes, we analyzed five genes, *TNF*, *LTA*, *NFKBIL1*, *ATP6V1G2*, and *BAT1*, in the SNP study and found three SNPs strongly associated with HCV-DCM; a T insertion at the position −421 of the *NFKBIL1* promoter (*NFKBIL1p*−421insT*) (OR = 4.25, $P = 0.003$, $Pc = 0.006$), an A to T substitution at the position +760 of the *ATP6V1G2* (*ATP6V1G2*+760T*) (OR = 4.25, $P = 0.003$, $Pc = 0.006$), and a fifth polymorphic haplotype (*BAT1p*05*) of the *BAT1* promoter (OR = 4.25, $P = 0.003$, $Pc = 0.006$) (Table 2). The *NFKBIL1p*−421insT* and *ATP6V1G2*+760T* are characteristic polymorphisms of the *NFKBIL1p*02* and *ATP6V1G2*3* alleles, respectively, which exhibited equivalent associations with HCV-DCM (Table 2). In contrast, neither *TNF* nor *LTA* polymorphisms showed significant association with HCV-DCM (data not shown).

Pairwise LD mapping around the candidate region in the Japanese population

Interestingly, the combination of the non-*HLA* gene alleles, consisting of *NFKBIL1p*02*, *ATP6V1G2*3*, and *BAT1p*05*, which were

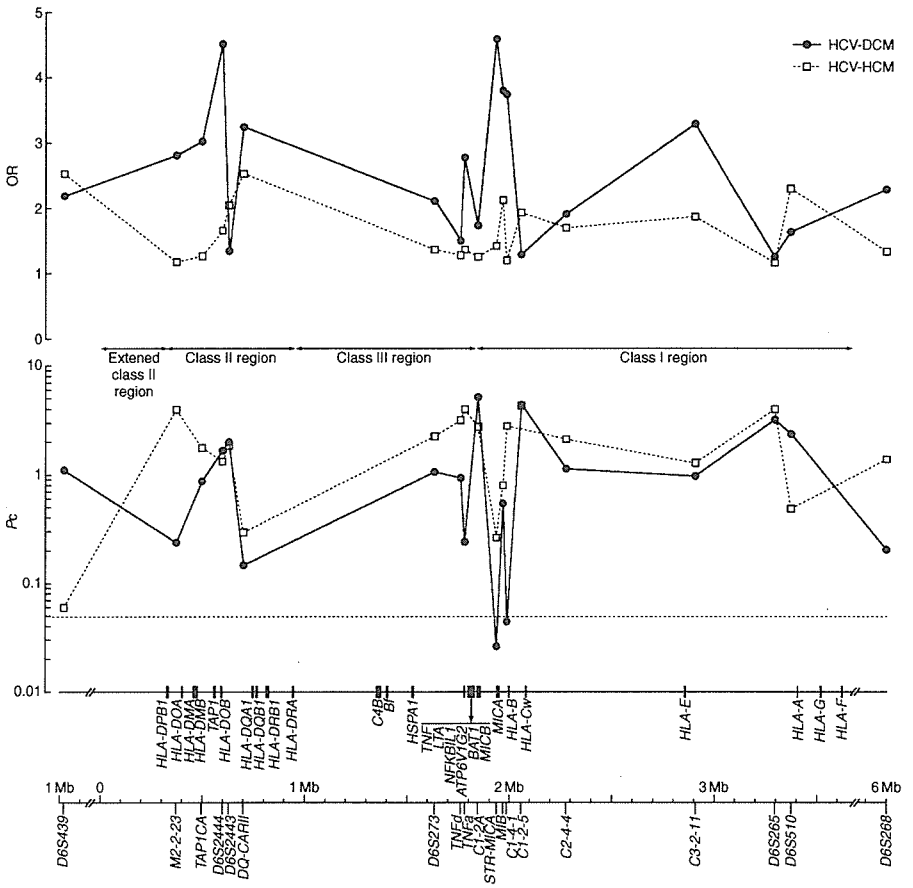

Fig. 1. **The susceptibility gene mapping for hepatitis C virus-associated dilated cardiomyopathy (HCV-DCM) and HCV-hypertrophic cardiomyopathy (HCV-HCM) with microsatellite markers throughout the human major histocompatibility complex genomic region.** Corrected *P* (*Pc*) value with logarithmic scale and odds ratio (*y*-axis) were plotted against physical location of the microsatellite markers on chromosome 6p21.3 (*x*-axis), their distance (in kb) in order from centromere to telomere. The dotted horizontal line shows the threshold for 5% significance after correcting for multiple testing.

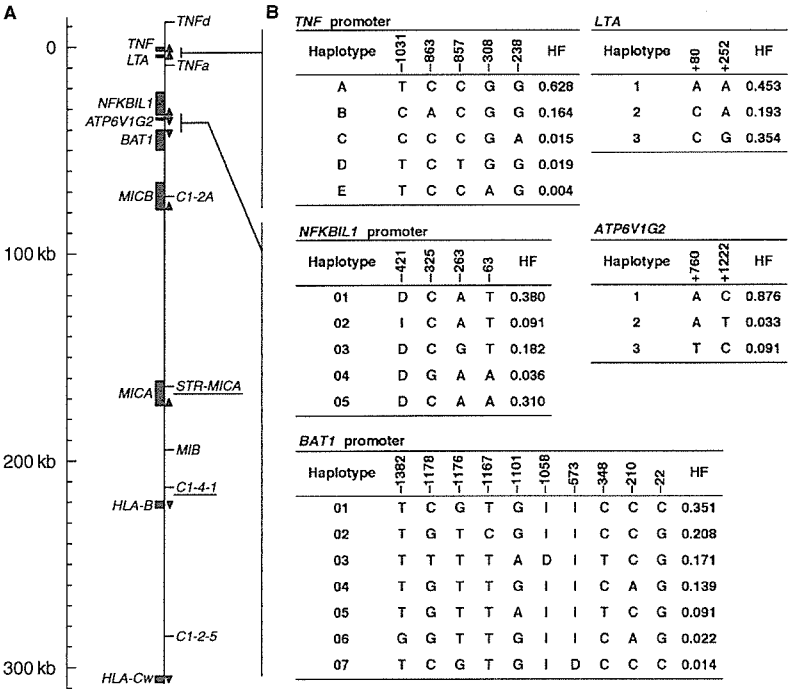

Fig. 2. **Candidate gene mapping in a susceptible 300-kb interval to hepatitis C virus-associated dilated cardiomyopathy (HCV-DCM).** (A) The physical map of candidate genes and genetic markers in the 300-kb interval. Microsatellite markers showing strong association with HCV-DCM in the microsatellite analyses were underlined. Arrow heads indicated the transcriptional direction of candidate genes. (B) Haplotype structures at the candidate gene loci. Haplotype frequencies (HF) were estimated by EM algorithms in the R package 'haplo.stats' (http://www.r-project.org/). Designations refer to the nucleotide position to transcriptional start site. Allelic sequences were defined by the same forward sequence as transcriptional direction in the genes. The I and D carried at *NFKBIL1p*−421*, *BAT1p*−1058*, and *BAT1p*−573* indicate the insertion and the deletion (indel), respectively. The indels carry allelic forms as follows (in order from 5′ to 3′): T/− at the *NFKBIL1p*−421*, AGG/− at the *BAT1p*−1058*, and CATCAGCTACCTCGGA/− at the *BAT1p*−573*.

significantly associated with HCV-DCM were tightly linked as a non-HLA haplotype block in a one-to-one correspondence in both patients and controls. This linkage was expected to result from a characteristic LD relationship in Japanese. We, therefore, evaluated the LD indexes for the specific LD block using other 15 polymorphic markers around the central MHC genomic region in the Japanese controls (Table 3). The pairwise LD mapping confirmed that these three alleles are in complete LD with each other, showing LD index being 1.0 for D' and 1.0 for r^2. In addition, *HLA-B*0702* was in strong LD not only with *HLA-Cw*0702* ($D' = 1.0$, $r^2 = 0.43$) but also with this non-HLA haplotype block ($D' = 1.0$, $r^2 = 0.59$).

The risk evaluation of the patient-shared block in HCV-DCM

We subsequently evaluated the non-HLA haplotype block as the main risk marker for HCV-DCM (Table 4). The analysis showed that a higher risk was conferred by *Hap A* (OR = 6.75, $P = 0.0003$, $Pc = 0.0081$) from the MHC class III – class I boundary region than by *Hap B* (OR = 3.96, $P = 0.02$, $Pc = 0.40$) from the MHC class I region. This strongly suggests that the disease susceptibility to HCV-DCM is controlled mainly by the non-*HLA* genes in the MHC class III – class I boundary region rather than by the classical *HLA* class I genes. The strong LD between *TNF* gene cluster and *NFKBIL1-BAT1* block also prompted us to examine a synergistic risk for HCV-DCM between *TNFp*A-LTA*1* and *NFKBIL1p*02-ATP6V1G2*3-BAT1*05-C1-2A*242-STR-MICA*183* by two-locus-analysis method of Svejgaard and Ryder (31). However, no synergistic risk between the haplotypes was found (data not shown). In light of location of the polymorphic markers composing of *Hap A*, the primary susceptibility locus could be narrowed down to approximately 133-kb interval between the *NFKBIL1* and *MICA* genes.

Discussion

It is well established that the *HLA* genes in the MHC have an important role in the regulation of immune response to acute and persistent HCV infection. The aim of this study was to investigate whether the non-*HLA* genes and *HLA* genes in the MHC might be associated with the susceptibility to HCV-DCM and/or HCV-HCM. Our MHC region-wide association study mapped the HCV-DCM susceptibility locus to the region spanning from *NFKBIL1* to *MICA* within the MHC class III – class I boundary region. In addition, the polymorphisms located around this boundary region were in LD with the classical *HLA-B* and *HLA-Cw* class I gene alleles. These observations suggest that the susceptibility to HCV-DCM may

Associations of candidate gene polymorphisms relevant to hepatitis C virus-associated dilated cardiomyopathy susceptibility within the central major histocompatibility complex region

	Genotype[a]									
	Cases (n = 21)			Controls (n = 120)			Carriers versus non-carriers			
Marker	++	+−	−−	++	+−	−−	OR	95% CI	P	Pc
Allele										
*NFKBIL1p*02*	1	8	12	0	18	102	4.25	1.57 - 11.54	0.003	0.014
*ATP6V1G2*3*	1	8	12	0	18	102	4.25	1.57 - 11.54	0.003	0.008
*BAT1p*05*	1	8	12	0	18	102	4.25	1.57 - 11.54	0.003	0.014
*HLA-B*0702*	0	6	15	0	11	109	3.96	1.28 - 12.29	0.022	0.356
*HLA-Cw*0702*	1	8	12	0	24	96	3.00	1.13 - 7.94	0.019	0.192
Polymorphism										
−421insT of *NFKBIL1*	1	8	12	0	18	102	4.25	1.57 - 11.54	0.003	0.005
+760T of ATP6V1G2	1	8	12	0	18	102	4.25	1.57 - 11.54	0.003	0.005

[a]++, homozygous carrier with the targeted polymorphisms; +−, heterozygous; −−, non-carrier

Table 2

be controlled by the non-*HLA* genes in LD with the *HLA* class I gene alleles rather than the *HLA* genes.

The mapped candidate susceptibility gene locus for HCV-DCM within the MHC class III – class I boundary region overlaps the susceptibility/resistance loci for some autoimmune diseases, such as rheumatoid arthritis (14) and insulin-dependent diabetes mellitus (32). Some candidate genes within the class III – class I boundary region that control the susceptibility to HCV-DCM encode molecules that are probably involved in immunity and inflammation. For example, *NFKBIL1* gene encodes a I-kappa-B-like molecule (33), which localizes within nuclear speckles (34). The product of *ATP6V1G2* gene responds to IL-1 as a subunit of vacuolar ATPase H^+ pump and modulates macrophage effector functions (35, 36). The role of the BAT1 proteins is less well defined, but they may act as negative regulators of an inflammatory cytokine (37) and effect cell proliferation in various human tissues including the heart (38). *MICA* and *MICB* genes exhibit a restricted expression pattern on cell in stress like those after viral infection (39–41) and may play a role in HCV infectious status as ligand of NKG2D (42, 43). These reported functions for the five non-*HLA* genes around the MHC class III – class I boundary region are helpful in explaining the genetic background of HCV-DCM, but cellular studies are clearly needed to determine the direct effect of HCV infection on the activity and the role of *NFKBIL1*, *ATP6V1G2*, *BAT1*, *MICB*, and *MICA* genes in the heart.

The candidate susceptibility locus identified in this study contained several functional SNPs, which might regulate transcriptional efficiency of the candidate genes. One such interesting SNPs is *NFKBIL1p*−62T/A* that lies within an E-box-binding motif (CANNTG) for transcriptional factors, E47 and USF1 (44). Second, the sequence spanning *BAT1p*−22G/C* (GCAGAT) and *BAT1p*−348C/T* (CCAT) is known to affect the *BAT1* expression via direct interaction with their transcriptional factors, Oct1 and YY1, respectively (45). These multiple functional polymorphisms may therefore combine functionally to increase the risk of DCM under the HCV infection. There were, however, still many ethnically characteristic and/or functionally unknown promoter polymorphisms other than the aforementioned SNPs. A transgenic mouse study revealed that the HCV-core protein is directly involved in the development of cardiomyopathy (46). The extent to which such polymorphisms influence the pathogenesis of HCV-DCM is a subject of further study.

Despite the same viral etiology, HCV involvement in cardiomyopathy can result in two distinct clinical outcomes, HCV-DCM and HCV-HCM, and a difference in the association with the MHC was revealed in this study. Whereas the microsatellite markers displayed a significant association of a particular MHC subregion with HCV-DCM, there was no significant association between the MHC and HCV-HCM. The HLA haplotypic markers in association with HCV-DCM are in strong LD with *B*0702-Cw*0702*, which are in LD with *DRB1*0101-DQB1*0501* in Japanese (47). However, these *HLA* alleles were not associated with HCV-associated liver diseases (22). In addition, a tendency toward severe HCV-infection status in Spanish whites was associated with *HLA-DR3-MICA-A4-HLA-B*18* (48); however, HCV-DCM patients in the present study showed

Pairwise linkage disequilibrium (LD) analysis of hepatitis C virus-associated dilated cardiomyopathy susceptibility loci for 120 Japanese individuals

		r^2														
	Locus	*TNFd*130*	*TNFp*A*	*LTA*1*	*TNFa*115*	*NFKBIL1p*02*	*ATP6V1G2*3*	*BAT1p*05*	*C1-2A*242*	*STR-MICA*183*	*MIB*336*	*C1-4–1*225*	*HLA-B*0702*	*C1-2-5*200*	*HLA-Cw* 0702*	*C2-4-4* 231*
	*TNFd*130*	–	0.19	0.23	0.30	0.14	0.14	0.14	0.52	0.01	0.04	0.07	0.09	0.01	0.06	0.03
	*TNFp*A*	0.46	–	0.00	0.04	0.05	0.05	0.05	0.15	0.01	0.06	0.01	0.03	0.04	0.00	0.01
	*LTA*1*	0.59	0.06	–	0.16	0.10	0.10	0.10	0.31	0.01	0.01	0.05	0.06	0.01	0.05	0.01
	*TNFa*115*	**0.95**	0.35	**0.85**	–	0.32	0.32	0.32	0.35	0.05	0.13	0.08	0.25	0.04	0.12	0.06
	*NFKBIL1p*02*	**1.00**	**1.00**	**1.00**	**0.86**	–	**1.00**	**1.00**	0.16	0.24	0.26	0.34	**0.59**	0.14	0.33	0.05
	*ATP6V1G2*3*	**1.00**	**1.00**	**1.00**	**0.86**	**1.00**	–	**1.00**	0.16	0.24	0.26	0.34	**0.59**	0.14	0.33	0.05
	*BAT1p*05*	**1.00**	**1.00**	**1.00**	**0.86**	**1.00**	**1.00**	–	0.16	0.24	0.26	0.34	**0.59**	0.14	0.33	0.05
D'	*C1-2A*242*	**0.85**	0.47	0.80	**0.87**	**0.90**	**0.90**	**0.90**	–	0.04	0.04	0.07	0.12	0.04	0.06	0.03
	*STR-MICA*183*	0.23	0.35	0.20	0.26	0.66	0.66	0.66	0.34	–	0.18	0.16	0.32	0.04	0.14	0.09
	*MIB*336*	0.46	**1.00**	0.26	0.50	0.55	0.55	0.55	0.39	0.53	–	0.34	**0.50**	0.10	0.21	0.01
	*C1-4-1*225*	0.66	0.45	0.69	0.40	0.62	0.62	0.62	0.54	0.50	0.60	–	**0.53**	0.08	**0.64**	0.06
	*HLA-B*0702*	**1.00**	**1.00**	**1.00**	**1.00**	**1.00**	**1.00**	**1.00**	**1.00**	**1.00**	**1.00**	**1.00**	–	0.23	**0.43**	0.05
	*C1-2-5*200*	0.18	0.55	0.16	0.21	0.61	0.61	0.61	0.28	0.25	0.46	0.43	**1.00**	–	0.06	0.12
	*HLA-Cw*0702*	0.55	0.10	0.61	0.46	0.67	0.67	0.67	0.46	0.44	0.49	**0.89**	**1.00**	0.34	–	0.11
	*C2-4-4*231*	0.22	0.11	0.08	0.57	0.79	0.79	0.79	0.30	0.79	0.40	**0.81**	**1.00**	0.77	**1.00**	–

Each polymorphic marker was positioned in order from major histocompatibility complex class III to class I subregion. The degree of LD is shown as the LD index of Lewontin correlation (D') in the lower left triangle and Pearson correlation (r^2) in the upper right triangle. Bold number indicates the strong LD: $D' > 0.8$, $r^2 > 0.4$. The solid LD block of genes from the class III region with the highest LD are boxed.

Table 3

Haplotype structures composed of significantly increased markers and single nucleotide polymorphisms (SNPs) in HCV-associated dilated cardiomyopathy

	Diplotype[a]									
	Cases (n = 21)			Control (n = 120)			Carriers versus non-carriers			
Haplotype	++	+−	−−	++	+−	−−	OR	95% CI	P	P_C
Hap A (MHC class III – class I boundary region side)										
*NFKBIL1p*02-ATP6V1G2*3-BAT1p*05-STR-MICA*183*	1	8	12	0	13	107	6.17	2.19 – 17.45	0.0005	0.0131
Hap B (MHC class I region)										
*B*0702-Cw*0702*	0	6	15	0	11	109	3.96	1.28 – 12.29	0.02	0.40

[a]++, homozygous carrier with the targeted haplotypes; +−, heterozygous; −−, non-carrier

Table 4

a different association with the *DRB1*0101-STR-MICA*183* (also known as *MICA-A5.1*)-*B*0702* haplotype. These haplotypic differences may indirectly reflect the genetic diversity among non-*HLA* genes that define each HLA haplotypes. Thus, these observations support the view that distinct genetic factors can affect the clinical outcome by regulating pathogenic pathway after the viral infection.

In summary, our susceptibility gene mapping showed that the non-*HLA* gene block consisting of the *NFKBIL, ATP6V1G2, BAT1, MICB*, and *MICA* genes within the MHC class III – class I boundary region was strongly associated with the susceptibility to HCV-DCM, whereas there was no significant association between the MHC genomic region and HCV-HCM. Through the disparity in the disease-associated HLA markers, we hypothesize that HCV-DCM and HCV-HCM have at least two distinct pathogenic mechanisms in relation to the MHC-meditated immune response, although the patients that developed DCM/HCM with HCV infection consisted of a small number of cases. Because the conclusions were based on the analysis of small number of patients, other independent studies with larger number of patients will be required. Nevertheless, our findings may provide an important clue as to the underlying cause of HCV-DCM in terms of immunogenetics. Because of tight LD among non-*HLA* alleles within the candidate genes, we could not identify specific susceptibility gene for HCV-DCM. Therefore, analysis of central MHC region in other Asian ethnic groups with HCV-DCM may contribute to a delineation of primary locus to the HCV-DCM susceptibility. Genome-wide microsatellite association studies in a much larger sample of infected patients will be also required to comprehensively understand their genetic background and the effect of genetic diversity on the outcome of HCV-associated cardiomyopathies.

References

1. Higuchi M, Tanaka E, Kiyosawa K. Epidemiology and clinical aspects on hepatitis C. *Jpn J Infect Dis* 2002: **55**: 69–77.
2. Mayo MJ. Extrahepatic manifestations of hepatitis C infection. *Am J Med Sci* 2003: **325**: 135–48.
3. Yan FM, Chen AS, Hao F et al. Hepatitis C virus may infect extrahepatic tissues in patients with hepatitis C. *World J Gastroenterol* 2000: **6**: 805–11.
4. Matsumori A, Matoba Y, Sasayama S. Dilated cardiomyopathy associated with hepatitis C virus infection. *Circulation* 1995: **92**: 2519–25.
5. Matsumori A, Matoba Y, Nishio R et al. Detection of hepatitis C virus RNA from the heart of patients with hypertrophic cardiomyopathy. *Biochem Biophys Res Commun* 1996: **222**: 678–82.
6. Takeda A, Sakata A, Takeda N. Detection of hepatitis C virus RNA in the hearts of patients with hepatogenic cardiomyopathy. *Mol Cell Biochem* 1999: **195**: 257–61.
7. Teragaki M, Nishiguchi S, Takeuchi K et al. Prevalence of hepatitis C virus infection among patients with hypertrophic cardiomyopathy. *Heart Vessels* 2003: **18**: 167–70.
8. Matsumori A, Ohashi N, Hasegawa K et al. Hepatitis C virus infection and heart diseases: a multicenter study in Japan. *Jpn Circ J* 1998: **62**: 389–91.
9. Cooke GS, Hill AV. Genetics of susceptibility to human infectious disease. *Nat Rev Genet* 2001: **2**: 967–77.
10. Shiina T, Inoko H, Kulski JK. An update of the HLA genomic region, locus information and disease associations: 2004. *Tissue Antigens* 2004: **64**: 631–49.
11. Marsh SG, Albert ED, Bodmer WF et al. Nomenclature for factors of the HLA system, 2002. *Hum Immunol* 2002: **63**: 1213–68.
12. Robinson J, Waller MJ, Parham P et al. IMGT/HLA and IMGT/MHC: sequence databases for the study of the major histocompatibility complex. *Nucl Acids Res* 2003: **31**: 311–4.
13. Mungall AJ, Palmer SA, Sims SK et al. The DNA sequence and analysis of human chromosome 6. *Nature* 2003: **425**: 805–11.

14. Okamoto K, Makino S, Yoshikawa Y et al. Identification of I kappa BL as the second major histocompatibility complex-linked susceptibility locus for rheumatoid arthritis. *Am J Hum Genet* 2003: **72**: 303–12.
15. Ozaki K, Ohnishi Y, Iida A et al. Functional SNPs in the lymphotoxin-alpha gene that associated with susceptibility to myocardial infraction. *Nat Genet* 2002: **32**: 650–4.
16. Knight JC, Udalova I, Hill AV et al. A polymorphism that affects OCT-1 binding to the TNF promoter region is associated with severe malaria. *Nat Genet* 1999: **22**: 145–50.
17. Mira J. Association of TNF2, a TNF-alpha promoter polymorphism, with septic shock susceptibility and mortality: a multicenter study. *JAMA* 1999: **282**: 561–8.
18. Burch GH, Gong Y, Liu W et al. Tenascin-X deficiency is associated with Ehlers-Danos syndrome. *Nat Genet* 1997: **17**: 104–8.
19. Ahmad T, Neville M, Marshall SE et al. Haplotype-specific linkage disequilibrium patterns define the genetic topography of the human MHC. *Hum Mol Genet* 2003: **12**: 647–56.
20. Walsh EC, Mather KA, Schaffner SF et al. An integrated haplotype map of the human major histocompatibility complex. *Am J Hum Genet* 2003: **73**: 580–90.
21. Stenzel A, Lu T, Koch WA et al. Patterns of linkage disequilibrium in the MHC region on human chromosome 6p. *Hum Genet* 2004: **114**: 377–85.
22. Kuzushita N, Hayashi N, Moribe T et al. Influence of HLA haplotypes on the clinical courses of individuals infected with hepatitis C virus. *Hepatology* 1998: **27**: 240–4.
23. Research Committee on Idiopathic Cardiomyopathy, the Ministry of the Health and Welfare, Japan. Guidelines for the diagnosis of idiopathic cardiomyopathy. In: *Annual Report of the Research Committee on Idiopathic Cardiomyopathy, the Ministry of the Health and Welfare, Japan*, 1985: 13–5 (in Japanese).
24. The WHO, /ISFC task force on the definition and classification of cardiomyopathies. Report of the WHO/ISFC task force on the definition and classification of cardiomyopathies. *Br Heart J* 1980: **44**: 672–3.
25. Foissac A, Salhi M, Cambon-Thomsen A. Microsatellites in the HLA region: 1999 update. *Tissue Antigens* 2000: **55**: 477–509.
26. Cullen M, Malasky M, Harding A, Carrington M. High-density map of short tandem repeats across the human major histocompatibility complex. *Immunogenetics* 2003: **54**: 900–10.
27. Higuchi T, Seki N, Kamizono S et al. Polymorphism of the 5′-flanking region of the human tumor necrosis factor (TNF)-alpha gene in Japanese. *Tissue Antigens* 1998: **51**: 605–12.
28. Allcock RJ, Baluchova K, Cheong KY, Price P. Haplotypic single nucleotide polymorphisms in the central MHC gene IKBL, a potential regulator of NF-kappaB function. *Immunogenetics* 2001: **52**: 289–93.
29. Wong AM, Allcock RJ, Cheong KY, Christiansen FT, Price P. Alleles of the proximal promoter of BAT1, a putative anti-inflammatory gene adjacent to the TNF cluster, reduce transcription on a disease-associated MHC haplotype. *Genes Cells* 2003: **8**: 403–12.
30. Knight JC, Keating BJ, Kwiatkowski DP. Allele-specific repression of lymphotoxin-alpha by activated B cell factor-1. *Nat Genet* 2004: **36**: 394–9.
31. Svejgaard A, Ryder LP. HLA and disease associations: detecting the strongest association. *Tissue Antigens* 1994: **43**: 18–27.
32. Yamashita T, Hamaguchi K, Kusuda Y . IKBL promoter polymorphism is strongly associated with resistance to type 1 diabetes in Japanese. *Tissue Antigens* 2004: **63**: 223–30.
33. Albertella MR, Campbell RD. Characterization of a novel gene in the human major histocompatibility complex that encodes a potential new member of the I kappa B family of proteins. *Hum Mol Genet* 1994: **3**: 793–9.
34. Semple JI, Brown SE, Sanderson CM et al. A distinct bipartite motif is required for the localization of inhibitatory kappaB-like (IkappaBL) protein to nuclear speckles. *Biochem J* 2002: **361**: 489–96.
35. Conboy IM, Manoli D, Mhaiskar V, Jones PP. Calcineurin and vacuolar-type H+-ATPase modulate macrophage effector functions. *Proc Natl Acad Sci USA* 1999: **96**: 6324–9.
36. Brisseau GF, Grinstein S, Hackam DJ et al. Interleukin-1 increases vacuolar-type H+-ATPase activity in murine peritoneal macrophages. *J Biol Chem* 1996: **27**: 2005–11.
37. Allcock RJ, Williams JH, Price P. The central MHC gene, BAT1, may encode a protein that down-regulates cytokine production. *Genes Cells* 2001: **6**: 487–94.
38. Leaw CL, Ren EC, Choong ML. Hcc-1 is a novel component of the nuclear matrix with growth inhibitory function. *Cell Mol Life Sci* 2004: **61**: 2264–73.
39. Groh V, Bahram S, Bauer S et al. Cell stress-regulated human major histocompatibility complex class I gene expressed in gastrointestinal epithelium. *Proc Natl Acad Sci USA* 1996: **93**: 12445–50.
40. Zwirner NW, Dole K, Stastny P. Differential surface expression of MICA by endothelial cells, fibroblasts, keratinocytes, and monocytes. *Hum Immunol* 1999: **60**: 323–30.
41. Molinero LL, Fuertes MB, Girart MV et al. NF-kappa B regulates expression of the MHC class I-related chain A gene in activated T lymphocytes. *J Immunol* 2004: **173**: 5583–90.
42. Karacki PS, Gao X, Thio CL et al. MICA and recovery from hepatitis C virus and hepatitis B virus infections. *Genes Immun* 2004: **5**: 261–6.
43. Jinushi M, Takehara T, Tatsumi T et al. Autocrine/paracrine IL-15 that is required for type I IFN-meditated dendritic cell expression of MHC class I-related chain A and B is impaired in hepatitis C virus infection. *J Immunol* 2003: **171**: 5423–9.
44. Boodhoo A, Wong AM, Williamson D et al. A promoter polymorphism in the central MHC gene, IKBL, influences the binding of transcription factors USF1 and E47 on disease-associated haplotypes. *Gene Exp* 2004: **12**: 1–11.
45. Price P, Wong AM, Williamson D et al. Polymorphisms at positions -22 and – 348 in the promoter of the BAT1 gene affect transcription and the binding of nuclear factors. *Hum Mol Genet* 2004: **13**: 967–74.
46. Omura T, Yoshiyama M, Hayashi T et al. Core protein hepatitis C virus induces cardiomyopathy *Circ Res* 2005: **96**: 148–50.
47. Saito S, Ota S, Yamada E, Inoko H, Ota M. Allele frequencies and haplotypic associations defined by allelic DNA typing at HLA class I and class II loci in the Japanese population. *Tissue Antigens* 2000: **56**: 522–9.
48. López-Vázquez A, Rodrigo L, Miña-Blanco A et al. Extended human leukocyte antigen haplotype EH18.1 influences progression to hepatocellular carcinoma in patients with hepatitis C virus infection. *J Infect Dis* 2004: **189**: 957–63.

Genotypes at chromosome 22q12-13 are associated with HIV-1-exposed but uninfected status in Italians

Yasuyoshi Kanari[a], Mario Clerici[b], Hiroyuki Abe[a], Hiroyuki Kawabata[a], Daria Trabattoni[b], Sergio Lo Caputo[c], Francesco Mazzotta[c], Hironori Fujisawa[d], Atsuko Niwa[a], Chiaki Ishihara[e], Yumiko A. Takei[f] and Masaaki Miyazawa[a]

Objective: Despite multiple and repeated exposures to HIV-1, some individuals possess no detectable HIV genome and show T-cell memory responses to the viral antigens. HIV-1-reactive mucosal IgA detected in such uninfected individuals suggests their possible immune resistance against HIV. We tested if the above HIV-1-exposed but uninfected status was associated with genetic markers other than a homozygous deletion of the *CCR5* gene.

Methods: Based on our mapping in chromosome 15 of a gene controlling the production of neutralizing antibodies in a mouse retrovirus infection, we genotyped 42 HIV-1-exposed but uninfected Italians at polymorphic loci in the syntenic segment of human chromosome 22, and compared them with 49 HIV-1-infected and 47 uninfected healthy control individuals by a closed testing procedure.

Results: A significant association was found between chromosome 22q12-13 genotypes and a putative dominant locus conferring anti-HIV-1 immune responses in the exposed but uninfected individuals. Distributions of linkage disequilibrium across chromosome 22 also differed between the exposed but uninfected and two other phenotypic groups.

Conclusions: The data indicated the presence of a new genetic factor associated with the HIV-1-exposed but uninfected status.

AIDS 2005, **19**:1015–1024

Keywords: HIV-1, exposed seronegatives, genetic background, chromosome 22, neutralizing antibody, synteny, association study

Introduction

The absence of clinical progression in some HIV-1-infected individuals and the lack of a detectable HIV-1 genome despite multiple and repeated exposures to this virus in some groups of people are noteworthy phenomena when considering the development of preventative and therapeutic means to HIV infection [1–3]. There are individuals who show strong HIV-1 antigen-specific T-lymphocyte responses and HIV-1-reactive mucosal IgA production despite the absence of detectable plasma HIV-1 RNA and HIV-1 cDNA from peripheral blood mononuclear cells (PBMC) [4–6]. HIV-1-neutralizing activity exerted by the IgA isolated from some HIV-1-exposed but uninfected individuals (EUI) [7–9] has suggested a possible contribution of the

From the [a]Department of Immunology, Kinki University School of Medicine, Osaka-Sayama, Osaka, Japan, the [b]Department of Immunology, DISP LITA Vialba, Milano University Medical School, Milano, Italy, the [c]Infectious Diseases Unit, Ospedale Santa Maria Annunziata, Firenze, Italy, the [d]The Institute of Statistical Mathematics, Tokyo, Japan, the [e]Department of Laboratory Animal Sciences, School of Veterinary Medicine, Rakuno Gakuen University, Ebetsu, Japan, and the [f]Department of Pathology, Tohoku University School of Medicine, Sendai, Japan.

Correspondence to M. Miyazawa, Department of Immunology, Kinki University School of Medicine, 377-2 Ohno-Higashi, Osaka-Sayama, Osaka 589-8511, Japan.

E-mail: masaaki@med.kindai.ac.jp.

Received: 26 August 2004; revised: 27 January 2005; accepted: 2 February 2005.

ISSN 0269-9370 © 2005 Lippincott Williams & Wilkins

host immune responses to the resistance against HIV infection. However, genetic factors that may influence the observed T-cell priming and the production of anti-HIV-1 IgA without the establishment of HIV replication are currently unknown.

Host genetic factors influencing viral entry and replication and antiviral immune responses have been extensively studied in mouse models of retroviral infections, among which the best analyzed is Friend mouse leukemia virus complex (FV) [10–13]. Host gene loci that control the entry and replication of FV in the target cells have been identified [14–17]. In addition, MHC class II loci directly restrict the T-helper cell recognition of the viral antigens [18–20], while a class I locus influences the production of cytokines from virus-specific T cells [21]. Another locus that has been mapped to chromosome 15 strongly influences the persistence of viremia after FV infection [12,22–25]. However, the possible relationship between the above persistence of viremia and production of virus-neutralizing antibodies has not been directly examined. Here we have performed linkage analyses on a mouse locus that influences the production of virus-neutralizing antibodies upon FV infection. An extension of this mouse study unexpectedly led us to find human chromosomal markers that are associated with the presence of HIV-1-reactive immune responses in HIV-uninfected individuals.

Methods

Mice, virus, and assays for neutralizing antibodies

B10.A and A/WySn mice were purchased from Japan SLC, Inc., Hamamatsu, Japan and The Jackson Laboratory, Bar Harbor, Maine, USA, respectively. The F_1 crosses and backcross mice were bred and maintained at Rakuno Gakuen University and Kinki University School of Medicine under specific pathogen-free conditions. The following experiments were approved by and performed under guidelines of each university. FV was prepared and inoculated as described [18,20–27]. FV-neutralizing antibodies were titered by immunoenzymatically visualizing foci of virus infection as described [20,26,27].

Analyses of simple sequence length polymorphisms (SSLP) and linkage mapping in mice

Genomic DNA was prepared from the tail tip of each mouse using DNeasy Tissue Kit (QIAGEN GmbH, Hilden, Germany). A pair of oligonucleotide primers for each microsatellite locus was designed based on the sequence information listed in the Genetic and Physical Maps of the Mouse Genome site (http://www-genome.wi.mit.edu/cgi-bin/mouse/) and ordered from QIAGEN GmbH. Fifty nanogrmas of each template DNA was subjected to 35 cycles of PCR amplification using a recombinant *Taq* polymerase (Invitrogen Life Technologies, Carlsbad, California, USA). PCR products were separated by electrophoresis in 4% agarose gel and visualized by ethidium bromide staining. Correlation between genotypes at each examined locus and the presence or absence of virus-neutralizing antibodies was analyzed by Pearson's χ^2 test. Map orders of the chromosomal loci and log-of-the-odds (LOD) scores were determined by multipoint analyses using MAPMAKER/EXP version 3.0b (The Whitehead Institute, Massachusetts, USA).

EUI and HIV-1-infected individuals

Forty-two heterosexual couples discordant for HIV-1 serostatus were enrolled. The female partner was HIV-1-infected in 32 couples, whereas the male partner was HIV-1-infected in the remaining 10 couples. The diagnosis of HIV-1 infection was made based on the detection of plasma HIV-1 RNA before the initiation of antiretroviral drug treatment and significant titers of serum anti-HIV-1 IgG antibody as described in the following section. The inclusion criteria for the EUI group were a history of multiple unprotected sexual episodes for >4 years with an average of eight reported unprotected sexual contacts per year (range 5 to >40) at the time of inclusion, and at least three episodes of at-risk intercourses within 4 months prior to the study point. Forty-two of the 49 HIV-1-infected individuals studied here are the steady and reportedly monogamous partners of the above EUI individuals. In all the infected individuals the diagnosis of HIV-1 infection was made during their chronic phase, and thus unprotected sexual intercourses had been initiated long before their diagnosis. Mean CD4 cell count of the infected partners at the time of this study was 370×10^6/l (range 36×10^6–850×10^6/l). Seven additional age- and sex-matched HIV-1-infected individuals were added to the study, and their HIV-related phenotypes were within the ranges of the above infected partners. All the EUI and HIV-1-infected individuals and 47 uninfected, age- and sex-matched healthy volunteers were enrolled from the Santa Maria Annunziata Hospital, Firenze, and the Luigi Sacco Hospital, Milano. All of the enrolees are Caucasians from the Toscana region. The ethics committees of the above hospitals have approved the research protocols. The genotyping analyses were approved by Kinki University School of Medicine. Written informed consent was obtained from all enrolees, and samples were anonymized and analyzed in a blinded fashion.

Phenotype definitions

Plasma HIV-1 load was quantified by using the AMPLICOR HIV Monitor test (Roche Diagnostic Systems, Nutley, New Jersey, USA) as described [4,6]. Possible presence of HIV-1 cDNA in PBMC and in cells

isolated by urethral swabbing or uterine cervical brushing was analyzed by a reverse transcription-PCR method [4,6]. For the detection of mucosal anti-HIV-1 IgA, 500 μl of mucus was collected from each enrolee by swabbing from the urethra or vagina [4,6]. Titers of serum anti-HIV antibodies were determined by an enzyme-linked immunosorbent assay (EIA) using Abbot HIV-1/2^+ test (Abbott Laboratories, Abbott Park, Illinois, USA). This assay detects HIV-specific IgG and IgM [7]. Titration of HIV-1-specific IgA in the mucosal secretions was performed by an isotype-specific EIA using the HIV EIA test (Calypte Biomedical Corp., Berkeley, California, USA) with modifications [4–9]. HIV-1-reactive memory T cells in the peripheral blood were enumerated by an enzyme-linked immunospot assay for interferon (IFN)-γ as described [6].

Analyses of human SSLP markers

Five-hundred nanograms of genomic DNA extracted from PBMC of each examined individual was used as the template for 40 cycles of PCR amplification using the flanking primer sets designed based on the sequence data compiled in the Ensembl Genome Browser (http://www.ensembl.org/) and ordered from QIAGEN GmbH. Each forward primer was labeled with a florescent dye, and 50–100 fmol of PCR amplified fragments were applied onto an ABI 3100 DNA sequencer (Applied Biosystems, Foster City, California, USA) with appropriate size markers. Peak identification and size measurements were done with the GeneScan software (Applied Biosystems). To determine absolute fragment sizes, PCR products obtained from two or more homozygotes for each locus were cloned into pCR2.1-TOPO vector (Invitorogen Life Technologies) and sequenced by using the M13 forward primer until six or more identical clones were observed for each allele.

Population genetic analyses and detection of linkage disequilibrium (LD)

Genotypic data were analyzed for possible population differentiation and LD between pairs of loci by using the Arlequin 2.001 (Genetics and Biometry Laboratory, University of Geneva, Switzerland). A population-pairwise genetic distance test using pairwise F_{ST} and extended exact test were performed to examine possible population differentiation. A likelihood ratio test was performed to examine the possible LD between pairs of loci. A total of 100,172 permutations on 10 initial conditions were performed by the expectation maximizing algorithm for each pair of loci.

Statistical analyses

Distributions of allele frequencies at each examined locus were compared between each pair of the three phenotypic groups by a Monte-Carlo approach using the CLUMP software [28]. T2 statistic was chosen because many cells in the contingency tables contained values ≤ 2.

To examine the possible presence of a dominant allele having different frequencies between the three phenotypic groups, mathematical analyses were performed based on the assumption that the number of individuals possessing each genotype had a multinominal distribution. Since the number of candidate dominant alleles was more than one, multiple comparisons were taken into consideration. The test statistics for alleles i and j, t_i and t_j, respectively, can be strongly correlated especially when most of the individuals having allele i or j are of the genotype i/j. Therefore, the typically used Bonferroni correction may be too conservative. A universally applicable method for overcoming this problem is a closed testing procedure [29], where t_i is based on a well-acquainted variance stabilizing transformation and the test statistic for a common hypothesis is based on the maximization of t_i's. To calculate the P-values, we applied a parametric bootstrap [30] based on the asymptotic null distribution of t_i's. Details of the mathematical methods are described in the Appendix section.

Results

Linkage mapping of a mouse locus controlling FV-neutralizing antibodies

When (B10.A × A/WySn)F_1 and A/WySn mice that share FV-susceptible *Fv-1*$^{b/b}$, *Fv-2*^{s}, and H2$^{a/a}$ genotypes were tested for their production of virus-neutralizing antibodies, none possessed a detectable level of neutralizing antibodies at post-infection day (PID) 10. Neutralizing antibodies remained undetectable at PID 15 and 20 in parental A/WySn mice. In contrast, all the infected (B10.A × A/WySn)F_1 mice possessed a significant neutralizing titer at PID 15, and the titers increased toward PID 20 (Fig. 1a). Therefore, possible segregation of neutralizing titers in (B10.A × A/WySn) × A/WySn backcross mice was examined by testing them at PID 15, 17, and 21. Virus-neutralizing antibodies were not detectable in 63 (44%) of the 143 backcross mice at PID 15 (Fig. 1b), suggesting that a single locus is involved in the production or lack of production of neutralizing antibodies. For linkage analyses, we concentrated genotyping on chromosome 15, because initial analyses performed by using 43 separate backcross individuals showed significant correlation between virus-neutralizing titers at PID 17 and genotypes at four loci in chromosome 15 (data not shown). The results of linkage analyses performed by using the 143 backcross mice indicated a strong correlation between genotypes at marker loci in chromosome 15 and titers of virus-neutralizing antibodies at PID 15, with the strongest correlation ($\chi^2 = 74.0$, $P = 1.17 \times 10^{-7}$) observed at the D15Mit71 locus (Fig. 2). Linkage mapping with MAPMAKER/EXP located a single locus determining the presence or absence of virus-neutralizing antibodies at PID 15

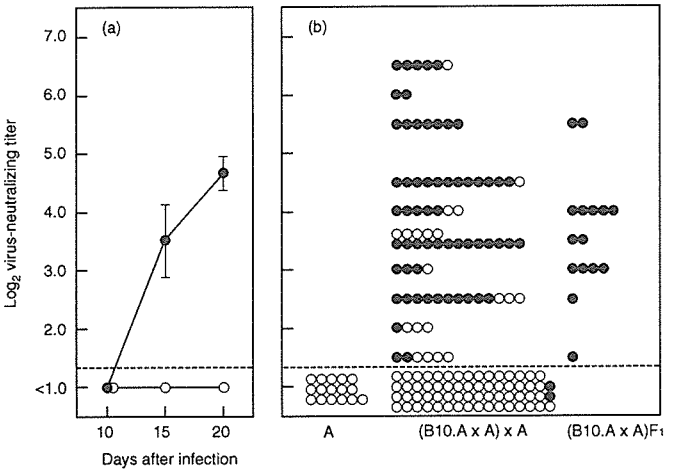

Fig. 1. Titers of virus-neutralizing antibodies in FV-infected mice. (a) Changes in the average titer ($n = 11-16$) of virus-neutralizing antibodies in (B10.A × A/WySn)F_1 (●) and A/WySn (○) mice at different time-points after infection with 150 spleen focus-forming units of FV. SEM. are shown with the bars. The dashed line indicates the limit of detection. (b) Titers of virus-neutralizing antibodies in each individual mouse tested at PID 15. Genotypes at the D15Mit71 locus are either homozygous for the A/WySn-derived allele (○) or heterozygous for the B10.A-derived and A/WySn-derived alleles (●).

between the D15Mit71 and D15Mit171 loci. Further mapping was performed by genotyping the backcross animals that possessed a critical recombination between the D15Mit28 and D15Mit171 loci. As a result, eight backcross mice that possessed reciprocal recombination within this region were identified (Fig. 2). Since a significant correlation ($P = 0.029$ by two-tailed Fisher's exact test) between genotypes at the D15Mit71, D15Mit2, D15Mit214, D15Mit69, and D15Mit70 loci and the production of virus-neutralizing antibodies at PID 15 was observed in these recombinant animals, it is conceivable that the locus controlling the production of FV-neutralizing antibodies is located within the region telomeric to the D15Mit1 and centromeric to D15Mit118 loci at the widest estimation.

Genetic analyses of HIV-1-exposed and uninfected Italians

The above region of mouse chromosome 15 harbors previously mapped genes that are known or likely to affect immune cell development and/or activation and retroviral replication. Therefore, we next explored the possibility that a putative ortholog of the above mouse locus might influence immune responsiveness in HIV-1 infection. Because of the route of transmission of HIV-1 and resultant rarity of multicase families, linkage analyses comparing affected and unaffected siblings are impossible. Thus, we performed a simple association study by comparing genotypes between the exposed but uninfected and HIV-1-infected individuals, hypothesizing that efficient anti-HIV-1 immune responses are associated with the presence of a dominant genetic factor which might be an ortholog of the above mouse locus conferring the ability to produce FV-neutralizing antibodies. Thus, the three phenotypically distinct groups of individuals (Table 1) were genotyped at the loci shown in Fig. 2. The examined groups were not different to each other when tested for population-pairwise genetic distance ($P > 0.17$), in accordance with their all being Caucasians enrolled from the Toscana region of Italy. When allele frequencies were compared among the three phenotypic groups, their distribution at the D22S277 locus differed between the EUI and healthy control groups at $P = 0.0396$. No significant difference was observed at the other loci. When likelihood ratio tests were performed for all possible pairs of the examined loci, a highly significant LD of an exact $P < 0.0004$ level was observed in all three groups between the D22S284, D22S423, and D22S299 loci, reflecting their close physical locations (Fig. 2 and Fig. 3). A similarly significant LD ($P < 0.00002$) was observed between the D22S418 and D22S1166 loci in all three groups, confirming their close genetic locations. Interestingly, a highly significant LD ($P < 0.00002$) was observed between the D22S276 and the above surrounding loci in both the HIV-1-infected and healthy control groups, but this was not observed in the EUI group (Fig. 3).

When frequencies of individuals possessing a particular allele at a given locus were compared among the three phenotypic groups by adopting a dominant model, objective mathematical analyses revealed multiple loci with significant differences (Table 2). These individual

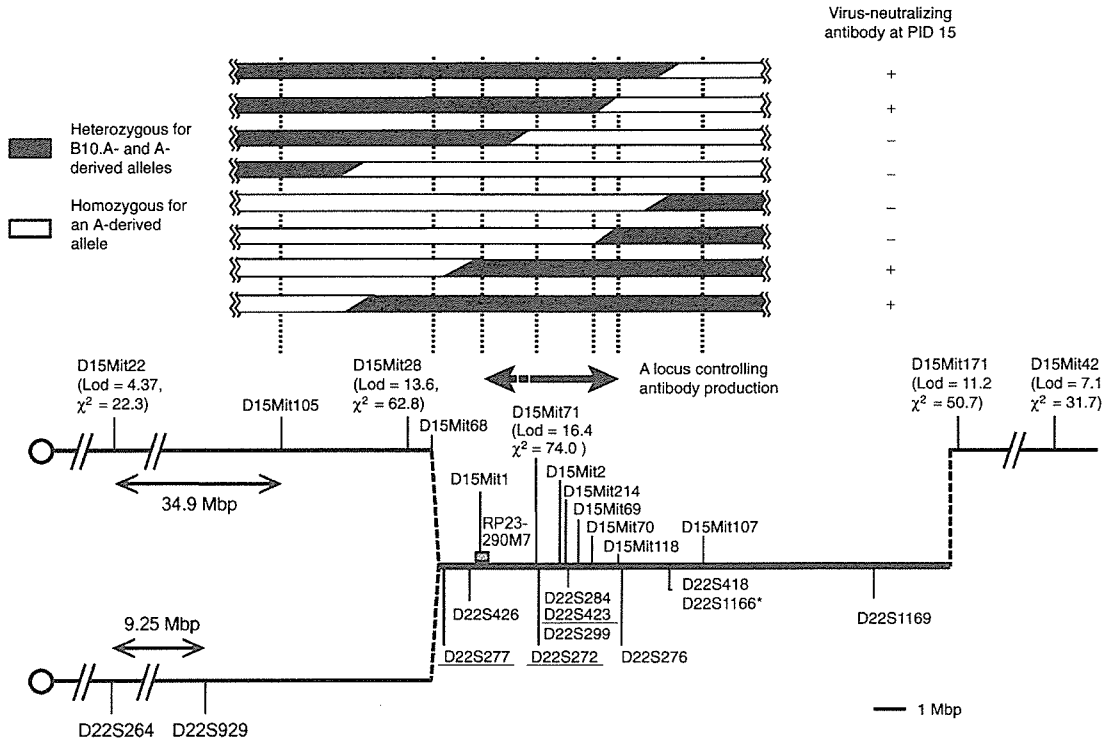

Fig. 2. The order of and distance between microsatellite markers located within the syntenic region of mouse chromosome 15 (the upper half of the diagram) and human chromosome 22 (the bottom half). Physical mapping and synteny data are based on those compiled in the Ensembl Genome Browser (http://www.ensembl.org/). Centromeres (○) are placed on the left. The mouse marker D15Mit28 has not been physically mapped, but genetic linkage data archived in the Mouse Genome Informatics site (http://www.informatics.jax.org) indicate that this locus, mapped at 43.7 cM, is closely linked to the D15Mit68 locus at 44.1 cM. Note that, although D15Mit1 is currently not included in the physical map of the mouse genome archived in the Ensembl Genome Browser, we identified the flanking primer and repeat sequences of this microsatellite marker (base numbers 47915-48097) within a clone of bacterial artificial chromosome, RP23-290M7, harbouring the segment of mouse chromosome 15 (shown with the hatched box). Lod scores and χ^2 values indicating degrees of genetic association between the identified genotypes and virus-neutralizing titers at PID 15 for each examined mouse locus are shown in parentheses. The estimated location of the putative mouse locus controlling the production of FV-neutralizing antibodies is shown with the bidirectional arrow. Human loci at which genotypes were compared between the EUI, HIV-infected, and healthy control groups are also shown, and the loci at which significant genetic differences were observed by the closed testing procedures are underlined. *The D22S1166 locus has not been physically mapped, but the genetic maps archived at the Center for Medical Genetics, Marshfield Clinic Research Foundation (http://research.marshfieldclinic.org/genetics/) indicate that this and the D22S418 loci are closely linked.

differences were further examined for possible false rejection of a single equal-frequency hypothesis due to multiple comparisons by using the closed testing procedure. As a result, frequencies of individuals possessing either the allele 156 or 158 at the D22S277 locus were significantly different between the EUI and two other groups, those of the individuals possessing the allele 134 at the D22S272 locus were significantly different between the EUI and healthy control groups, and those of individuals possessing the allele 229 at the D22S423 locus also differed significantly between the EUI and HIV-infected individuals.

Discussion

In the present study we have demonstrated that the presence or absence of virus-neutralizing antibodies in FV-infected (B10.A × A/WySn) × A/WySn backcross mice at PID 15 is closely associated with their genotypes at the chromosome 15 loci. The linkage mapping data indicated that a single gene controlling the production of virus-neutralizing antibodies was located near the D15Mit71 locus, colocalizing with the previously mapped *Rfv-3* locus [23,24]. Since the *Rfv-3*-associated phenotypes were defined by clearance of viremia by

Table 1. HIV-1-related phenotypes of the three groups genetically analyzed in the present study.

Group	Age	Plasma HIV load (copies/ml)	Urethral/ vaginal anti-HIV-1 IgA ($A_{405\ nm}$)	Serum anti-HIV-1 IgG ($A_{405\ nm}$)	HIV-1 envelope-reactive IFN-γ ELISPOT[a] (/10^6 cells)
HIV-1-exposed but uninfected ($n = 42$)	40.1 ± 1.4	Not detectable (all)[b]	0.556 ± 0.047[c] (0.12–1.14)[d]	0.004 ± 0.0006 (0.00–0.02)	131.2 ± 11.3[e] (5–280)
HIV-1-infected ($n = 49$)	40.8 ± 1.9	<40 – 750,000 (median: 400)[f]	0.360 ± 0.039 (0.11–0.87)	0.793 ± 0.069 (0.11–1.25)	63.4 ± 9.2 (<5–120)
Healthy control ($n = 47$)	37.8 ± 3.6	Not detectable (all)[b]	0.002 ± 0.0006 (0.00–0.03)	0.002 ± 0.0001 (0.00–0.01)	<5 (<5–15)

Numbers shown are mean ± SEM except for the Plasma HIV load.
[a]PBMC were stimulated with a mixture of five synthetic peptides representing the immunodominant and promiscuous epitopes identified in the HIV-1 gp160 [6], and spots of secreted interferon (IFN)-γ were visualized and counted by using a biotin-conjugated anti-IFN-γ antibody.
[b]All enrolees were tested for the presence of HIV genome by measuring plasma HIV-1 RNA and by detecting HIV-1 cDNA from total RNA of peripheral blood mononuclear cells. In the case of the exposed uninfected individuals (EUI), possible presence of HIV-1 cDNA was also tested in mucosal cells by reverse transcription–PCR. All the individuals in the EUI and healthy control groups were negative for all these tests.
[c]Significantly higher than the average for the HIV-1-infected individuals at $P = 0.0022$ by Welch's t test. A non-parametric analysis by Mann–Whitney's U-test also showed a significant difference, $P = 0.021$.
[d]Ranges of observed values are shown in parentheses for IgA and IgG titers and enzyme-linked immunospot (ELISPOT) foci.
[e]Significantly higher than the average for the HIV-1-infected individuals at $P = 0.015$ by Welch's t test, and $P = 0.0002$ by Mann–Whitney's U-test.
[f]All the HIV-1-infected individuals were enrolled during their chronic phase of infection before the initiation of antiretroviral drug treatment, but 32 of the 42 infected partners and the seven additional HIV-1-infected enrolees were receiving the highly active anti-retroviral therapy at the time of this study. The range of plasma viral load in the 13 currently untreated individuals in the infected group was 5900 to 750 000 (median, 65 000) copies/ml.

35–40 days after FV infection [22–25], and neutralizing antibodies were detectable at as early as PID 15 in mice possessing the B10.A-derived dominant allele (Fig. 1), it is conceivable that early production of virus-neutralizing antibodies is associated with early clearance of viremia.

It is intriguing that genotypes at microsatellite loci located within the segment of human chromosome 22 syntenic to mouse chromosome 15 differed between the HIV-1-exposed but uninfected and HIV-1-infected groups of individuals. The strongest association was observed at the D22S423 locus where the frequency of individuals possessing the allele 229 was significantly higher in the EUI group than in the HIV-1-infected one even after corrections for multiple comparisons were made. This marker locus is located in the middle of the chromosomal segment corresponding to the region of mouse chromosome 15 that harbors the gene locus controlling the production of virus-neutralizing antibodies (Fig. 2). It may also be worth noting that the alleles 156 and 158 at the D22S277 locus that are rare (5.6 and 9.3% per haploid chromosome, respectively) among the Caucasian CEPH

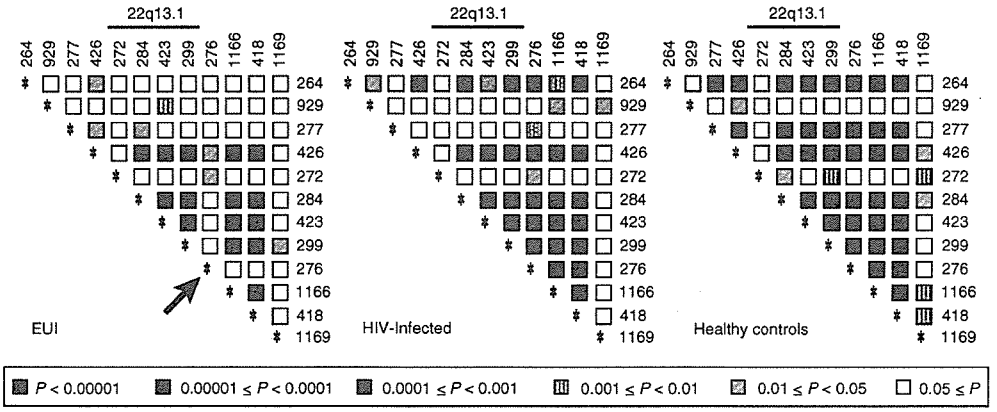

Fig. 3. Distributions of LD across chromosome 22. LD is plotted for the 12 microsatellite loci examined against each other, each represented by a small square. Locus names are abbreviated by omitting D22S. The pattern of distribution of LD is shown for each of the three phenotypic groups for comparison. Filling patterns reflect the significance level in exact P values as indicated at the bottom. The arrow indicates observed disruption within the segment of multilocus LD in the EUI group. The allele distributions in the three examined groups did not deviate from the Hardy-Weinberg equilibrium at any examined locus, except only at the D22S418 locus in the healthy control group, when exact tests using a Markov chain (100,172 chain length and 1,000 dememorization steps) were performed.

Table 2. Chromosome 22q association analyses.

Cytogenetic location	Locus	Allele size (bp)	Frequency in the EUI group[a]	Compared to[b]	Odds ratio	*P* value	
						Individual hypothesis	Common hypothesis
22q11.21	D22S264	188	0.405	HIV	3.276	0.0142	ns[c]
		198	0.238	HC	0.306	0.0128	ns
22q12.2	D22S277	158	0.310	HIV	3.766	0.0152	ns
		156 or 158	0.429	HIV	3.656	0.0066	0.0378[d]
				HC	3.875	0.0079	0.0448[d]
		162	0.262	HC	0.379	0.0371	ns
22q13.1	D22S272	134	0.667	HC	0.308	0.0243	0.0466[d]
22q13.1	D22S423	229	0.333	HIV	4.200	0.0087	0.0317[d]
22q13.2	D22S418	145	0.605	HC	2.520	0.0475	ns
	D22S1166	130	0.571	HC	2.816	0.0266	ns
22q13.32	D22S1169	126	0.643	HC	2.528	0.0313	ns

[a]Frequencies of individuals possessing the indicated allele either heterozygously or homozygously.
[b]HIV, HIV-1-infected individuals; HC, Healthy controls.
[c]Not significant (ns) at the $P < 0.05$ level.
[d]These differences are also significant ($P < 0.05$) after conventional Bonferroni correction.

population [31,32] were more frequently observed in the EUI group (9.5 and 17.9%, respectively). There were significant differences in the frequency of the allele 156 and that of the allele 158 ($P = 0.035$ and 0.0061, respectively, by two-tailed Fisher's exact test) when the HIV-1-infected and healthy control groups were combined and compared with the EUI group. The rates of microsatellite mutation are much higher than those of point mutation at coding genes [33], and the most common stepwise mutation is biased toward the reduction of repeat numbers for microsatellites of >20 repeats [34]. Thus, we can justifiably hypothesize that the alleles 156 and 158 at the D22S277 locus (25 and 26 dinucleotide repeats, respectively) are both linked to the same putative allele that is associated with the presence of immune responses to HIV-1 in the uninfected individuals. In this regard, the variance stabilizing analyses performed by assuming that the alleles 156 and 158 are both linked to a single dominant genetic factor resulted in the demonstration of significant differences between the EUI and HIV-1-infected, and the EUI and healthy control groups, and these individual null hypotheses were also rejected (significant difference validated) after the correction for multiple comparisons was made (Table 2). Further, when the same comparison was made between a combined group of the HIV-1-infected and healthy control individuals and the EUI group, the frequency of individuals possessing either the allele 156 or 158 was significantly higher among the EUI ($P = 0.0019$), and this was highly significant even after the correction for multiple comparisons was made ($P = 0.0121$). The combination of the HIV-1-infected and healthy control groups was justifiable because neither allele frequency distributions nor frequencies of individuals possessing the allele 156 or 158 were significantly different between the two groups. Thus, genotypes at multiple loci within the segment of human chromosome 22 that is syntenic to mouse chromosome 15 are significantly associated with the presence of strong mucosal and T-cell immune responses against HIV-1 (Table 1) in HIV-uninfected Italians. Furthermore, the multilocus LD spanning from D22S284 to D22S418 which is observed in both the HIV-infected and healthy control groups is disrupted at the D22S276 locus in the EUI group (Fig. 3). This observation is consistent with the hypothesis that in the ancestors of the EUI individuals a possible recombinational or mutational event might have happened in the chromosomal segment surrounding this locus.

Production and class-switching of virus-neutralizing antibodies in FV-infected mice are dependent on CD4 T-cell functions [26,27,35], and the priming of CD4 T-helper cells with a singe-epitope peptide resulted in the early production and class-switching of virus-neutralizing antibodies and strong protection against FV infection [20,27]. Likewise, EUI individuals enrolled into the present study possessed significantly higher amounts of mucosal anti-HIV-1 IgA and larger numbers of HIV-1 envelope-reactive T cells in the peripheral blood in comparison with the HIV-infected individuals (Table 1). IgA antibodies isolated from some EUI individuals have been shown to inhibit the replication of primary HIV-1 isolates [7] and HIV-1 transcytosis across the epithelial cells *in vitro* [8,36]. Thus, it is possible that efficient priming of T cells with HIV antigens might have resulted in rapid production of HIV-1-reactive IgA antibodies which, in turn, might have been involved in the possible immune protection in the EUI individuals. In this regard, it is noteworthy that IFN-γ production is required for the control of viremia and class-switching of virus-neutralizing antibodies in FV infected mice [37].

It has been shown that CD4 T cell-dependent early IgA responses against influenza virus infection can be generated in the absence of virus-specific IgM and IgG [38], and costimulatory signals required for mucosal IgA production are strikingly different from those needed for systemic antibody responses [39]. Similarly, mucosal IgA